Stability and electronic structure of ultrathin [001] $(GaAs)_m(AlAs)_m$ superlattices

D. M. Wood, S.-H. Wei, and Alex Zunger
Solar Energy Research Institute, Golden, Colorado 80401
(Received 3 June 1987; revised manuscript received 16 November 1987)

The general issues of stability towards disproportionation or disordering of $(AC)_m(BC)_m$ superlattices are addressed by simple model calculations based on detailed first-principles results for the $(GaAs)_1(AlAs)_1$ [001]-orientation alternate-monolayer superlattice. Valence-force-field (VFF) calculations permit isolation of strain-related contributions to the superlattice formation energy and a simple electrostatic energy model highlights the importance of charge transfer in stabilizing or destabilizing such ordered phases. We predict that bulk $(GaAs)_1(AlAs)_1$ is in fact unstable with respect to disproportionation into zinc-blende constituents because of insufficient Ga-Al charge transfer. Epitaxial growth on GaAs or AlAs simply makes this structure less unstable. A simple semiquantitative model for [001] $(AC)_1(BC)_1$ extracted from detailed self-consistent calculations makes clear the competition between (destabilizing) strain effects and (potentially stabilizing) charge transfer effects. We extract trends for thicker superlattices with the aid of VFF calculations and generalizations of the electrostatic model. We find that unstable thin superlattices become (per bond) less unstable as the repeat period increases, while stable ones become less stable per bond. Kinetic factors or surface effects must be invoked to explain the spontaneous occurrence of $(GaAs)_m(AlAs)_m$ structures. The electronic structure of $(GaAs)_1(AlAs)_1$ is analyzed in detail and interpreted in terms of simple distortions and band folding of the virtual-crystal-approximation band structure.

I. INTRODUCTION

Recent perfection[1-9] of atomic-scale control over nucleation and growth using modern crystal-growth techniques such as molecular-beam and liquid-phase epitaxy and chemical-vapor deposition has made possible laboratory synthesis of ultrathin-layer structures $(AC)_m(BC)_n$, consisting of m layers of the binary compound AC alternating with n of BC along a specified growth direction. Like ordinary bulk compounds, experimentally-synthesized ultrathin superlattices of compound semiconductors, including the extreme case of alternate monolayer structures, e.g., $(GaAs)_1(AlAs)_1$ (Refs. 2 and 3), $(GaSb)_1(AlSb)_1$ (Ref. 4), $(GaAs)_1(InAs)_1$ (Refs. 5 and 6), $(GaAs)_1(InAs)_3$ and $(GaAs)_3(InAs)_1$ (Ref. 7), $(GaAs)_1(GaSb)_1$ (Ref. 8), and $(GaP)_n(InP)_n$ (Ref. 9), exhibit a high degree of crystalline order,[10] exceedingly small room-temperature interlayer diffusion coefficients,[11] maximum order at a particular growth temperature [e.g., $\sim$840 K for[12] $(GaAs)_1(AlAs)_1$], and an order-disorder transformation above a critical temperature [e.g.,[13] 820–880 K for $(GaAs)_1(AlAs)_1$]. These experimental manifestations of order are highlighted by the recent observation that $(GaAs)_1(AlAs)_1$,[3] $(InAs)_1(GaAs)_3+(InAs)_3(GaAs)_1$,[7(a)] $(InAs)_1(GaAs)_1$,[6] $(GaAs)_1(GaSb)_1$ (Ref. 8), and $(InP)_n(GaP)_n$ (Ref. 9) all grow *spontaneously* as an ordered compound $A_nB_{4-n}C_4$ $(1\le n\le 3)$ even under continuous growth conditions, without artificially imposing a layer-by-layer structure, and that $(GaAs)_1(InAs)_1$ (Refs. 5 and 6), $(GaSb)_1(AlSb)_1$ (Ref. 4), and $(GaAs)_1(GaSb)_1$ (Ref. 8) form *ordered* structures even though the analogous *disordered* alloys $Ga_xIn_{1-x}As$, $Ga_xAl_{1-x}Sb$, and $Ga_xAs_{1-x}Sb_x$ are known to have a miscibility gap. Although superlattices are routinely fabricated and used in devices, it has generally not been known whether they are thermodynamically *stable*, or represent instead *metastable* states (made accessible, for instance, by a non-equilibrium growth technique) separated by large activation barriers from lower-energy configurations.

Consider the issues of stability with respect to disproportionation into the constituents $(AC)_m(BC)_n \rightarrow m(AC)+n(BC)$ and with respect to disordering $(AC)_m(BC)_n \rightarrow A_xB_{1-x}C$. It is convenient to define the formation enthalpy of a perfectly ordered compound $A_mB_nC_{m+n}$ in structure α per $2(m+n)$ atoms as its energy $E^\alpha[A_mB_nC_{m+n}]$ relative to that of equivalent amounts of its binary constituents at their respective equilibria:

$$\Delta H^\alpha[A_mB_nC_{m+n}]=E^\alpha[A_mB_nC_{m+n}]-mE[AC]-nE[BC]\ . \quad (1)$$

For a disordered (D) $A_xB_{1-x}C$ alloy of composition x one similarly defines the mixing enthalpy

$$\Delta H^D(x)=E[A_xB_{1-x}C]-xE[AC]-(1-x)E[BC]\ . \quad (2)$$

The Gibbs free energy of formation of the perfectly ordered phase is then

$$\Delta G^\alpha[A_mB_nC_{m+n}]=\Delta H^\alpha[A_mB_nC_{m+n}]-T\Delta S^\alpha\ , \quad (3)$$

where ΔS^α is the difference in (electronic plus vibration-

al) entropy between the ordered phase and the binary constituents, while the disordered alloy has a free energy of formation

$$\Delta G^D(x,T)=\Delta H^D(x)-T\,\Delta S^D(x)\ , \tag{4}$$

where $\Delta S^D(x)$ includes electronic and vibrational as well as configurational[14] contributions. In what follows we will examine the stability of perfectly ordered superlattices, using the notation (m,n) to denote the $(AC)_m(BC)_n$ ordered (O) superlattice (rather than the structure label α). The following are the possibilities at $T=0$.

(I) *Ordered superlattice stable:* $\Delta H^O(m,n)<0$ (i.e., stable with respect to disproportionation) and $\Delta H^O(m,n)<\Delta H^D(x_m)$ (stable with respect to disordering), where $x_m=m/(m+n)$. There are two subcases: (a) $\Delta H^D(x_m)\leq 0$. This is the case for most compound-forming metallurgical systems (e.g.,[15] Cu-Au), as well as for ternary $A_nB_{4-n}C_4$ nonisovalent semiconductor compounds, e.g., chalcopyrites.[16] (b) $\Delta H^D(x_m)\geq 0$. *All* isovalent pseudobinary semiconductor alloys $A_xB_{1-x}C$ have[17,18] $\Delta H^D(x)\geq 0$ whether or not they order at lower temperatures. However, $\Delta H^D(x_m)>0$ and $\Delta H^O(m,n)<0$ has been predicted for[19,20] SiC, ferromagnetic[21] $(CdTe)_1(MnTe)_1$, epitaxial[19] SiGe (grown on Si), and possibly[22] for $(GaP)_1(InP)_1$. In either case Ia or Ib the ordered phase is absolutely stable at low enough temperature; as the temperature rises, the alloy entropy $\Delta S^D(x)$ increases faster than[14] $\Delta S^\alpha(x)$ and an order-disorder transition can occur.[16]

(II) *Ordered superlattice metastable:* $0<\Delta H^O(m,n)<\Delta H^D(x)$. The disordered alloy can develop a miscibility gap at finite temperature, and it is then possible that the superlattice is more stable than the single-phase disordered alloy[22,23] (and is observable) $\Delta G^O<\Delta G^D$, but may be less stable than a two-phase (AC- and BC-rich) disordered alloy (hence, it will disappear given enough time or annealing). This is likely to be the case[22,23] for systems showing superlattice ordering inside the miscibility gap, e.g.,[8] $(GaAs)_1(GaSb)_1$, and has been predicted[24(a),24(b)] for Ag-Au.

(III) *Ordered superlattice unstable:* $\Delta H^O(m,n)>\Delta H^D(x_m)$. In this case the superlattice will not order at any temperature, since even at $T=0$ the disordered alloy has a smaller enthalpy. Since $\Delta S^D>\Delta S^O$ because of configurational entropy,[14] in this case the alloy is further stabilized as the temperature is increased. Srivastava *et al.*[25] have shown that this situation does not occur for isovalent semiconductor alloys with an appreciable lattice mismatch between constituents AC and BC (where $\Delta H^D\geq 0$) since ordered phases accommodate the associated strain better than do disordered phases, hence $\Delta H^O<\Delta H^D$. For small lattice mismatch, however, $\Delta H^O>\Delta H^D>0$ is possible.

The exceedingly low atomic diffusion constants of cold (i.e., room-temperature) semiconductors[11] suggest that the mere existence of ordered superlattices can be consistent with any of the above, since activation barriers to phase transformations may be insurmountable on laboratory time scales.

The thermodynamic properties of perhaps the best-studied superlattice, $(GaAs)_m(AlAs)_n$, exhibit a delicate energy balance between strain destabilization and potential stabilization by charge transfer: it has a lattice mismatch[26] $\Delta a\equiv a_{AlAs}-a_{GaAs}=0.0009$ Å at its growth temperature ~ 800 K (hence, an ordered phase would offer but a small reduction in strain energy), yet Ga and Al differ in electronegativity (hence, charge transfer could stabilize it). This delicacy is highlighted by the disparate views on the stability of the alternating monolayer $(GaAs)_1(AlAs)_1$ superlattice. Kuan *et al.*,[3] who observed the ordered superlattice in continuous growth, characterized it as the equilibrium state of $Ga_xAl_{1-x}As$, as did Petroff, who suggested[27] the layer-by-layer grown superlattice represents the low-energy equilibrium phase. On the other hand, Phillips[28] suggested that this phase is intrinsically unstable but is stabilized due to pinning by oxygen impurities, and Ourmazd and Bean[29] speculated it was stable only due to the extrinsic effect of substrate strain.

Theoretical estimates of the formation enthalpy $\Delta H^O(1,1)$ of the monolayer superlattice [Eq. (1)] similarly range (referring all energies to a primitive cell of four atoms) between predicted stability (-1.5 meV, from empirical tight binding;[30] -20 meV, in a Hartree-Fock cluster calculation after optimization of bond lengths[31]) and instability ($+15.5$,[32] $+35$,[33] and $+21.2$ meV,[34] all using self-consistent pseudopotentials; and ~ 0 using low-order perturbation theory about the uniform electron gas[35]).

We have performed first-principles pseudopotential and all-electron total-energy calculations for $(GaAs)_1(AlAs)_1$ in the [001] orientation and suggest this system to belong to class III above (unstable at $T=0$ with respect to disordering, and unstable with respect to disproportionation). We examine the dependence of semiconductor superlattice stability on (i) the properties of the AC and BC constituents, (ii) superlattice structural parameters, (iii) the mode of growth (bulk or epitaxial), and (iv) superlattice thickness. We also present a simple conceptual picture by which trends for systems other than $(GaAs)_1(AlAs)_1$ may be understood, and simple models which semiquantitatively describe the first-principles results. We also examine the changes in electronic band structure in going from the zinc-blende constituents to the ordered $(GaAs)_1(AlAs)_1$ superlattice by way of a fictitious $Ga_{0.5}Al_{0.5}As$ virtual-crystal alloy. A brief description of these results has appeared.[36]

II. STRUCTURE AND FORMATION ENTHALPY OF THE [001] ORIENTATION $(AC)_1(BC)_1$ SUPERLATTICE

A. Structure

An underlying theme below will be that $(AC)_n(BC)_n$ superlattices for small n's share a great deal in common with more familiar ordered ternary compounds. The chalcopyritelike[37] ABC_2 structure, for example, is identical to an $(AC)_2(BC)_2$ superlattice in the (2,0,1) orientation.[20] Similarly, in the $(GaAs)_1(AlAs)_1$ [001]-orientation superlattice[2,3] shown in Fig. 1(a) [space group $P\bar{4}m2$]

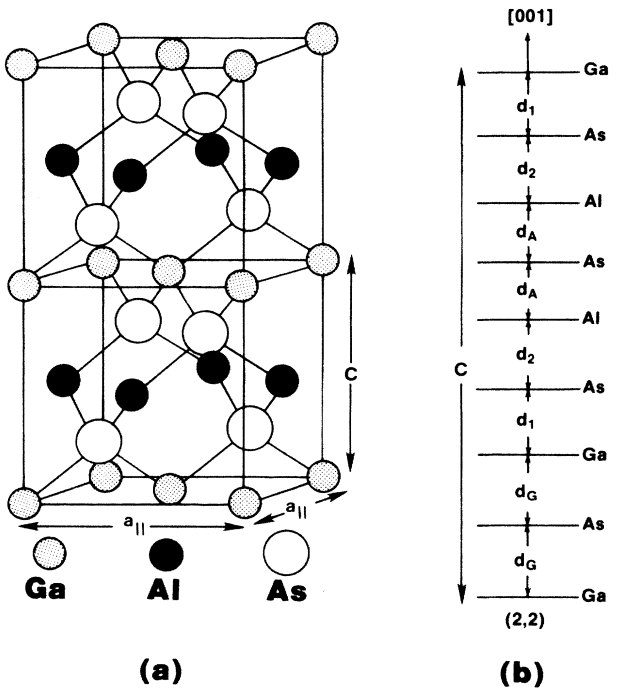

FIG. 1. (a) Two stacked unit cells of the [001]-orientation $(AC)_1(BC)_1$ superlattice; (b) structural parameters of simple model (Sec. VIII A) for $(AC)_m(BC)_m$ illustrated for $m=2$.

the cation sublattice forms a compound identical to the CuAu-I phase observed in metallurgy.[15,38] In the context of the phase diagram for an $A_xB_{1-x}C$ alloy, this is a member of the face-centered-cubic (fcc) Landau-Lifshitz structures[39] and (together with chalcopyrite[20,37] and[19,20] $L1_1$ CuPt structures) is thus a likely candidate for an ordered structure around $x=\frac{1}{2}$.

A tetragonal primitive cell and cell-internal atomic displacement parameters are hallmarks of most observed ternary adamantine phases.[37,40] In addition to the cell dimensions c and a, for which we define the tetragonal ratio $\eta \equiv c/a$, the $P\bar{4}m2$ structure is characterized by the anion displacement parameter u which measures, in units of c, the A-C interplanar spacing along the c axis:

$$u=\tfrac{1}{4}+(R_{AC}^2-R_{BC}^2)/\eta^2a^2 . \tag{5}$$

Here R_{AC} and R_{BC} are, respectively, the $A-C$ and $B-C$ bond lengths in this structure,

$$R_{AC}=a[\tfrac{1}{8}+\eta^2u^2]^{1/2},\quad R_{BC}=a[\tfrac{1}{8}+\eta^2(u-\tfrac{1}{2})^2]^{1/2} . \tag{6}$$

For $\eta=1$ and $u=\frac{1}{4}$ we recover $R_{AC}=R_{BC}=\sqrt{3}a/4$, the same relationship as in a cubic zinc-blende structure; this bond length generally differs from the *ideal* bond lengths of the pure binary compounds $d_{AC}^O=(\sqrt{3}/4)a_{AC}$ and $d_{BC}^O=(\sqrt{3}/4)a_{BC}$ of the binary constituents with equilibrium lattice constants a_{AC} and a_{BC}. This failure to accommodate ideal bond configurations results in microscopic strain.[19,20,25] Obviously one can accommodate any desired R_{AC} and R_{BC} (for example, d_{AC}^O and d_{BC}^O) by suitable choice of a and u [Eq. (6)] at the expense, however, of distortions of bond angles from the ideal tetrahedral value 109.5°. Conversely, one could achieve ideal bond angles at the expense of bond-length distortions. Unlike for zinc-blende or CuPt binary structures, it is impossible[19] in the lattice-mismatched $(AC)_1(BC)_1$ superlattice of Fig. 1(a) to simultaneously preserve "ideal" d_{AC}^O and d_{BC}^O bond lengths and perfect tetrahedral bond angles. The equilibrium structure hence represents a compromise with finite strain energy.

B. Formation enthalpy and the role of strain energy

The formation enthalpy [or, at zero pressure, the energy, Eq. (1)] of *bulk* $(AC)_1(BC)_1$ is simply its energy at equilibrium relative to equivalent amounts of its zinc-blende constituents at their respective equilibria, i.e., (per four atoms) with structural parameters explicitly displayed,

$$\Delta H^O(1,1)=E[(AC)_1(BC)_1,a_{\rm eq},u_{\rm eq},\eta_{\rm eq}] -E[AC,a_{AC}]-E[BC,a_{BC}] , \tag{7}$$

where all structural parameters adopt energy-minimizing (eq) values. Most superlattices are grown as an epitaxial layer on a thick substrate. Provided the thickness of the layer does not exceed the critical thickness for nucleation of misfit dislocations,[41] this situation corresponds to the constraint that superlattice dimensions parallel to the substrate-epilayer interface, denoted here with the subscript $\|$, coincide with substrate cell dimensions (i.e., the epitaxial layer is "registered" or "pseudomorphic"). On a substrate (s) of lattice constant a_s, the epitaxial formation enthalpy becomes[19,40]

$$\delta H^O(1,1;a_s)=E[(AC)_1(BC)_1,\ a_\|=a_s] -E[AC,\ a_\|=a_s]-E[BC,\ a_\|=a_s] , \tag{8}$$

where all structural parameters except $a_\|$ adjust to minimize the energy of each of the three phases. We may define the "substrate stabilization" energy $\Delta E_{\rm SS}$ as[40]

$$\Delta E_{\rm SS}^O(a_s)=\delta H^O(1,1;a_s)-\Delta H^O(1,1) . \tag{9}$$

For $\Delta E_{\rm SS}^O<0$, the epitaxial constraint destabilizes the epitaxially-grown superlattice less than it does its binary constituents, so that the epitaxial system is more stable (or less unstable) than its bulk-grown counterpart. We will examine the stability of bulk and epitaxial superlattices by calculating from first principles the quantities in Eqs. (7)–(9), minimizing the energies with respect to the structural parameters $\{a,u,\eta\}$ [Eqs. (5) and (6)].

III. METHOD OF CALCULATION

A. Hamiltonian and convergence

We have calculated for the $(GaAs)_1(AlAs)_1$ superlattice $\Delta H^O(1,1)$ of Eq. (7); $\delta H^O(1,1;a_s)$ [Eq. (8)] was calculated for $a_s=a_{\rm GaAs}$ and $a_s=a_{\rm AlAs}$. We use the first-principles pseudopotential total-energy method[42] within

the local-density-functional formalism and the Ceperley-Alder exchange-correlation functional as parametrized by Perdew and Zunger.[43] The proximity (~ 15 eV) of the Ga $4s$ and $3d$ levels on the scale of a typical III-V compound valence-band width, and the frozen-core approximation underlying the pseudopotential description, might raise questions about its reliability for systems containing Ga. We have therefore, as a check on the pseudopotential results, performed independent calculations for certain geometries in an all-electron approach, using the general-potential linear augmented-plane-wave (LAPW) method.[44] In this method all states are treated self-consistently with no frozen-core approximation; the Hedin-Lundqvist exchange-correlation functional[45] was used in the LAPW work.

In Table I we show nonrelativistic and semirelativistic all-electron atomic orbital energies and radii $\langle r_{nl} \rangle$ for Al, Ga, and As. We note that semirelativistic calculations result in a considerable lowering of s orbital energies of Ga and As (together with a contraction, as measured by $\langle r_{ns} \rangle$). We have hence used semirelativistic pseudopotentials (Fig. 2) in our calculation, generated by the prescription by Kerker,[46] which by construction precisely reproduce the all-electron atomic valence orbital energies and radii. For these nonsingular pseudopotentials we have used a plane-wave basis with a fixed kinetic-energy cutoff of 16 Ry, corresponding to ~ 310 basis functions for zinc-blende GaAs and AlAs, and ~ 620 basis functions for $(GaAs)_1(AlAs)_1$.

Given the delicate energetics of $(GaAs)_1(AlAs)_1$, high precision is required to reliably evaluate stability. $\Delta H^O(1,1)$ is the *difference* between energies for ordered phases of similar ground-state charge densities and electronic properties. Hence, if the superlattice and its binary constituents are treated *equivalently*, we expect systematic errors associated with the use of the local-density approximation will largely cancel in $\Delta H^O(1,1)$, leaving convergence errors as the principal source of error. Three distinct convergence criteria need to be controlled: (i) convergence with respect to the basis set size, (ii) adequate and consistent sampling of the Brillouin zone in evaluating charge densities and total energies, and (iii) the degree of self-consistency in the electronic potentials. We have examined convergence as follows. (i) *Basis functions:* We use variationally equivalent basis sets for the superlattice and its binary constituents by selecting equal kinetic-energy cutoffs in reciprocal space. At the average theoretical lattice constant of GaAs and AlAs for the relaxed superlattice, the formation enthalpy $\Delta H^O(1,1)$ changes [for the Brillouin-zone sampling described in (ii) below] by only 1.8 meV per four atoms (while the energy of the superlattice changes by ~ 48 meV) as the kinetic-energy cutoff for the plane-wave basis is changed from 16 to 18 Ry. (ii) *Brillouin-zone (BZ) sampling:* For both pseudopotential and LAPW calculations the two **k** points obtained by folding the two conventional Chadi-Cohen fcc special **k** points[47] into the smaller superlattice Brillouin zone were used, guaranteeing total energies of identical precision for the superlattice and its zinc-blende constituents.[48] At $a = 5.52$ Å we examined the variation in $\Delta H^O(1,1)$ as the special **k** points used for sampling were changed to a different set equivalent to 12 points evenly spaced along the z direction [obtained via unfolding of one special **k** point in the tetragonal Brillouin zone of a (6,6) superlattice]. $\Delta H^O(1,1)$ changed by only ~ 0.6 meV per four atoms although the superlattice energy changed by 112.5 meV. (iii) *Self-consistency:* The energy uncertainty in $\Delta H^O(1,1)$ associated with deviation from perfect self-consistency we estimate to be less than 0.5 meV per four atoms.

All of these convergence errors ($\lesssim 2$ meV) are much smaller than the physically relevant values of ΔH^O (~ 10's of meV per four atoms; see below).

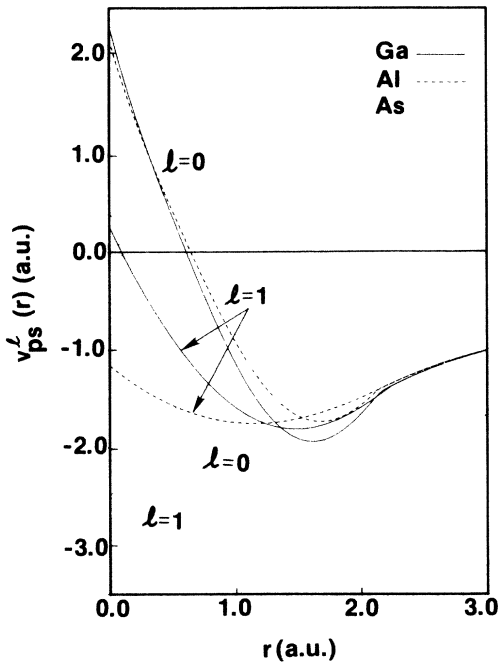

FIG. 2. Semirelativistic first-principles nonlocal pseudopotentials used in plane-wave basis calculations for $l = 0, 1$ for Ga, Al, and As.

TABLE I. Nonrelativistic (NR) and semirelativistic (SR) all-electron atomic orbital eigenvalues $\varepsilon_s, \varepsilon_p$ (eV) and orbital radii $\langle r_{ns} \rangle$, and $\langle r_{np} \rangle$ (a.u.) for Ga, Al, and As using the local-density approach with Ceperley-Alder (Ref. 43) exchange-correlation potentials.

	ε_s	$\langle r_{ns} \rangle$	ε_p	$\langle r_{np} \rangle$
		Ga		
NR	−8.93	2.37	−2.77	3.37
SR	−9.17	2.33	−2.74	3.37
		Al		
NR	−7.81	2.55	−2.80	3.44
SR	−7.84	2.53	−2.79	3.44
		As		
NR	−14.25	1.97	−5.38	2.55
SR	−14.70	1.93	−5.35	2.55

B. Superlattice structural parameters

Since the total energy of the superlattice is a function of the three parameters a, η, and u [Eq. (7)], many self-consistent first-principles calculations would be required to precisely find its equilibrium geometry. We have instead chosen to use Keating's[49] valence-force-field (VFF) method to establish geometries to be studied self-consistently within the local-density method. While the *value* of $\Delta H^O(1,1)$ obtained by first-principles calculations will be different from the VFF value,[25] the structural parameters will be very similar.[25] For semiconductors, the VFF method provides a natural bridge between continuum elasticity theory and a microscopic structural description, and permits identification of the strain contributions to formation energies. It is expected to be quite accurate since use of VFF predictions for atomic coordinates will lead to errors in the total energy (VFF or first principles) that are only of second order in the (small) errors in the coordinates. For GaAs and AlAs we have used the force constants tabulated by Martin;[50] fit to experimental phonon spectra, they reproduce very well bulk elastic properties and, e.g., observed bond lengths for dilute isovalent impurities in semiconductor hosts.[51] We have, however, used the equilibrium bond lengths R_{AC} and R_{BC} predicted by our first-principles calculations.[52]

IV. FIRST-PRINCIPLES RESULTS FOR GaAs, AlAs, $(GaAs)_1(AlAs)_1$, AND $Ga_{0.5}Al_{0.5}As$

A. Zinc-blende GaAs and AlAs

The calculated equilibrium properties of zinc-blende-structure GaAs and AlAs are summarized in Table II where they are compared with experiment[53–55] and with other first-principles calculations.[32–34,56,57] We note (i) the AlAs bond is stronger (has a larger cohesive energy), though slightly longer, than the GaAs bond; (ii) elastic properties, here the bulk modulus, are reasonably well reproduced by the calculations; and (iii) the small lattice mismatch between these materials (~ 0.01 Å extrapolated[53] to 0 K) is considerably exaggerated by the first-principles calculations: $\Delta a \simeq 0.087$ and -0.029 Å for the pseudopotential and LAPW methods, respectively.

The strain energy "frozen into" the unrelaxed $(AC)_1(BC)_1$ superlattice scales as $\bar{B}\bar{a}(\Delta a)^2$, where $\bar{a}$ is the average lattice constant of AC and BC (close to the equilibrium lattice parameter we find for the superlattice), Δa is the lattice mismatch, and $\bar{B}$ is the average bulk modulus of AC and BC. Hence pseudopotential calculations for the *unrelaxed* $(GaAs)_1(AlAs)_1$ structure may overestimate strain effects by a factor ~ 100 and the LAPW calculations by ~ 10. However, the accommodation (via relaxation of η and u) of the two distinct bond lengths will be sufficient to remove ~ 60–70% of this spurious strain energy [see Appendix A and Sec. VI A, Eq. (20)].

B. $(GaAs)_1(AlAs)_1$ superlattice

We examine $\Delta H^O(1,1)$ under three distinct structural situations, results for which are shown in Table III; all energies are per four atoms i.e., per ABC_2 formula unit. First (model I), given the extremely small *experimental* lattice mismatch Δa (Table II), we neglect lattice distortions ($u \neq \frac{1}{4}$, $\eta \neq 1$) that would result from a finite Δa, and take a_{eq} to be the average of the *calculated* lattice parameters (Table II), i.e., $a_{eq} \simeq \bar{a} = (a_{GaAs} + a_{AlAs})/2 = 5.560$ Å. The pseudopotential method (first line of Table III) yields $\Delta H^O(1,1) = +25.0$ meV; the LAPW method gives (at the *theoretical* average lattice constant $\bar{a} = 5.676$ Å) $\Delta H^O(1,1) = +12.5$ meV. This difference reflects almost entirely the larger lattice mismatch in the pseudopotential (PS) results. (Scaling the strain contribution ΔE_{VD} (see Sec. V A) by $[(\Delta a_{LAPW}/(\Delta a)_{PS}]^2 = (0.029/0.087)^2$, and adding ΔE_{CE} would find for the unrelaxed superlattice $\Delta H^0 = 12.3$ meV, in excellent agreement with the LAPW result given the radically different computational approach and the different exchange-correlation potentials used.)

TABLE II. Calculated pseudopotential (PS), all-electron LAPW, and experimental (Expt.) equilibrium lattice parameters (a, extrapolated to $T = 0$ K), bulk moduli (B) and cohesive energies (E_c) for zinc-blende GaAs and AlAs, compared with results of other calculations. NC: norm-conserving pseudopotential; SR: semirelativistic; NR: nonrelativistic; CA: Ceperley-Alder exchange-correlation (XC); HL: Hedin-Lundquist XC; W: Wigner XC; E denotes plane-wave basis kinetic-energy cutoff.

	GaAs			AlAs		
	a (Å)	B (GPa)	E_c (eV/atom)	a (Å)	B (GPa)	E_c (eV/atom)
PS	5.517	78.0	4.14	5.604	73.4	4.39
LAPW	5.690	76.2	3.88	5.661	76.1	4.33
a	5.609			5.725		
b	5.655	72.0	3.86	5.670	73.4	4.26
c	5.570	72.5		5.641	74.1	
d	5.617	81	3.7	5.670	86	4.1
e	5.58			5.61		
Expt.	5.642[f]	75.4[g]	3.31[h]	5.652[f]	~ 77[g]	3.81[h]

[a]Reference 34 (NC, SR, CA XC, $E \sim 13$ Ry).
[b]Reference 32 (NC, SR).
[c]Reference 56 (NC, NR, HL XC, $E = 12$ Ry).
[d]Reference 57 (NC, NR, W XC, $E \leq 10$ Ry).
[e]Reference 33 (NC, SR, CA XC, $E \sim 12$ Ry).
[f]Reference 53.
[g]Reference 54.
[h]Reference 55.

TABLE III. Calculated pseudopotential bulk and epitaxial formation enthalpies of $(GaAs)_1(AlAs)_1$. See text in Sec. IV B.

Model	a	η	u	$\Delta H^O(1,1)$	Conditions
I	5.560	1	$\frac{1}{4}$	+25.0	$\bar{a}$, unrelaxed
II	5.560	1.000	0.246	+21.3	$\bar{a}$, relaxed bulk
IIIa	5.517	1.015	0.246	+14.44[a]	a_{GaAs}, epitaxial
IIIb	5.604	0.985	0.246	+15.92[a]	a_{AlAs}, epitaxial

[a] $\delta H^O(a_s)$ for epitaxial cases (IIIa and IIIb).

The non-negligible lattice mismatch present in the *theoretical* calculations for GaAs and AlAs (Table II) suggests that, in order to realistically appraise superlattice stability, the different Ga—As and Al—As bond lengths should be accommodated within the structural description. In model II (second line of Table II) we therefore evaluate $\Delta H^O(1,1)$ at the *relaxed* $(a_{eq}, \eta_{eq}, u_{eq})$ values (5.560, 1.000, 0.246), found using valence-force-field results and the theoretical binary bond lengths. The net pseudopotential formation enthalpy (second line in Table III) $\Delta H^O(1,1)=+21.3$ meV differs from the all-electron result $\Delta H^O(1,1)=+9.5$ meV, evaluated at (5.676, 1.000, 0.252). The larger strain energy (due to the larger Δa) in the pseudopotential case accounts for about half of the discrepancy; the remainder is probably attributable to the freezing of core d electrons in the pseudopotential description. The ~4-meV relaxation (found using the pseudopotential method) is relatively small.

In model III we evaluate, using the pseudopotential method, the epitaxial formation enthalpy $\delta H^O(1,1;a_s)$ [Eq. (8)] using (GaAs (IIIa) and AlAs (IIIb) as substrates (last two lines of Table III). Using VFF predictions for η (for tetragonally-distorted GaAs and AlAs) and for η and u [for $(GaAs)_1(AlAs)_1$], we find $\delta H^O(1,1;a_{GaAs})=+14.4$ meV while $\delta H^O(1,1;a_{AlAs})=+15.9$ meV. ΔE_{SS} [Eq. (9)] is hence, respectively, -6.9 and -5.4 meV per four atoms for $(GaAs)_1(AlAs)_1$ on GaAs and AlAs as substrates. (These values of course reflect the large theoretical Δa; we find $\Delta E_{SS} \lesssim 0.1$ meV per four atoms using the experimental Δa.) Hence the conclusion that this (bulk or epitaxial) superlattice is unstable with respect to GaAs + AlAs remains unmodified, in contrast with the speculation of Ref. 29. We next estimate the relative stabilities of a *disordered* $Ga_{0.5}Al_{0.5}As$ alloy and the ordered $(GaAs)_1(AlAs)_1$ superlattice.

C. The random alloy and order-disorder transformations

The virtual-crystal approximation[58] (VCA) formed the basis of much early theoretical work on substitutionally-disordered $A_xB_{1-x}C$ pseudobinary alloys. It replaces the microscopically inhomogeneous distribution of A and B atoms with a lattice of identical fictitious atoms whose properties (e.g., pseudopotentials v_{ps}^l) represent a composition average of A and B. Using the same numerical parameters described in Sec. III A for the binary compounds, we performed self-consistent calculations for such a zinc-blende $Ga_{0.5}Al_{0.5}As$ alloy near its expected equilibrium lattice constant, $(a_{GaAs}+a_{AlAs})/2$. We find $\Delta H^D(x=\frac{1}{2})=+428$ meV per four atoms, a massive destabilization of the disordered phase with respect to either the phase-separated zinc-blende constituents or to the ordered bulk $[\Delta H^O(1,1)]$ or epitaxial $[\delta H^O(1,1;a_s)]$ superlattice. While in reasonable agreement with Oshiyama and Saito[34] (who find $\Delta H^D=352$ meV per four atoms), this energy poorly represents a disordered alloy since the total energy depends in a nonlinear way on the bare crystal potential (which is linearly averaged in a VCA calculation). Real disordered alloys are better described as a superposition of the five nearest-neighbor environments available in a tetrahedrally-coordinated compound (see Sec. VI and Appendix B). A more physically reasonable first-principles estimate of the formation energy of the random alloy has been given by Kunc and Batra,[33] who find from a calculation for a partially-disordered unit cell that ΔH^D for $Ga_{0.5}Al_{0.5}As$ lies about 60 meV per four atoms above ΔH^O of the ordered (1,1) superlattice. Insofar as electronic and vibrational contributions to the entropy are expected to be very similar[14] for the disordered alloy, the ordered superlattice, and the binary constituents, we retain only the configurational contributions to ΔS^D for the disordered alloy and set $\Delta S^O=0$. Taking the configurational contribution to the entropy ΔS^D of the $x=0.5$ random alloy to be $2k_B \ln 2$ per two cations[14] (four atoms), we estimate the maximum ordering temperature of the superlattice as

$$T^O \simeq [\Delta H^D(x=0.5)-\Delta H^O(1,1)]/(\Delta S^D-\Delta S^O) \simeq 229\,^\circ\text{C} .$$

Conversely, using an upper limit for T^O of 550 °C gleaned from the experimental work of Holonyak *et al.*[13] [who found Zn diffusion catalyzed disordering of $(GaAs)_m(AlAs)_n$ at $T \gtrsim 550\,^\circ$C] we infer [using our value $\Delta H^O(1,1)=21$ meV] $\Delta H^D(x=0.5)$ to lie about 98 meV per four atoms above $\Delta H^O(1,1)$. This yields $\Delta H^D(x=0.5)=119$ meV $=1.37$ kcal/1-cation mole, or an "interaction parameter" $\Omega=4\Delta H^D(x=\frac{1}{2})=5.5$ kcal/1-cation mole. This is considerably larger than experiment[59,60] and would predict a miscibility gap for this system at low enough temperatures. However, this estimate of Ω presents an upper limit for two reasons: (i) there is probably some local ordering (clustering) in the disordered alloy,[60(b)] *reducing* its entropy ΔS^D, and (ii) there is considerable disorder in the (experimental) or-

dered superlattice,[3] *increasing* its entropy ΔS^O. Each effect reduces the entropy change $\Delta S^D - \Delta S^O$ upon disordering, reducing the calculated Ω.

We conclude from the pseudopotential calculations described above that the energetic hierarchy for the $(GaAs)_1(AlAs)_1$-random alloy system at $T=0$ K (for $a_s = a_{GaAs}$ or a_{AlAs}) is

$$0 < \delta H^O(1,1;a_s) \lesssim \Delta H^O(1,1) < \Delta H^D(x=\tfrac{1}{2}) \ . \quad (10a)$$

i.e., this system belongs to class II described in the Introduction. However, using the description of Appendix B [Eq. (B1)] and the LAPW results, $\Delta E^{(n)}(Ga_nAl_{4-n}As_4) = +8.7, \ +11.5, \ +8.4$ for $n=1,2,3$, respectively (in meV per four atoms, all evaluated at the average *experimental* lattice constant), we find $\Omega = 4\Delta H^D(x=\frac{1}{2}) = 8.6$ meV $= 0.4$ kcal per 1-cation mole, in better agreement with experiment. Since the superlattice ($n=2$) is of higher energy $\Delta E^{(2)}$ than a mixture $\Delta H^D(x=\frac{1}{2})$ including other n's, we predict the more reasonable stability order

$$0 < \Delta H^D(x=\tfrac{1}{2}) < \Delta H^O(1,1) \ , \quad (10b)$$

i.e., class III of the Introduction.

Note that the maximum ordering temperature $T^O \lesssim 550\,^\circ$C observed by Holonyak and co-workers[13] for these superlattices is *below* the growth temperatures (600–800 °C) used by Kuan *et al.*,[3] who have observed partial ordering. This supports our conclusion that the stable thermodynamic state of the superlattice *at growth temperatures* is disordered, and hence the partial ordering observed may be *metastable* (we thank J. Van Vechten for discussion of this point). Note further that the positive value of ΔH^D suggests that a miscibility gap (MG) may exist at finite temperatures T_{MG} [where $d^2\Delta G/dx^2$ of Eq. (4) changes sign]. Bublik and Leikin[60(a)] estimated $T_{MG} \simeq 120\,^\circ$C, whereas Balzarotti *et al.*[60(b)] estimated $T_{MG} \simeq 90\,^\circ$C. These are well below conventional growth temperatures. The fact that spontaneous ordering[3] is observed above both T_{MG} and T^O hence suggests to us that this ordering is not mandated by *bulk* thermodynamics.

V. ANALYSIS OF THE SUPERLATTICE FORMATION ENTHALPY

A. Conceptual decomposition of superlattice formation enthalpy

Although ΔH^O for a given ordered phase determines thermodynamic stability at $T=0$ K, its value alone provides no insight into (i) how successfully the two distinct AC and BC bond lengths are accommodated, (ii) the nature of charge transfer attendant upon formation of the superlattice, and (iii) trends across a class of ternary ordered compounds of the same structure. For this reason we next describe a decomposition which permits isolation of these distinct physical trends.

In this process we imagine formation of an ordered phase to occur in three conceptual steps.[19,20,25] First, (i) compress (or dilate) the constituents AC and BC to the common lattice constant a_{eq} of the ordered ternary phase, generally intermediate between those, a_{AC} and a_{BC}, of AC and BC. This step ("volume deformation," VD) requires an energy *investment*

$$\Delta E_{VD} = \{E[AC,a_{eq}] - E[AC,a_{AC}]\} + \{E[BC,a_{eq}] - E[BC,a_{BC}]\} \ . \quad (11)$$

Since deformation of equilibrium structures is involved, $\Delta E_{VD} \geq 0$. Second, (ii) assemble the prepared (compressed or dilated) AC and BC units to form the ordered structure *without* relaxing the structural parameters (i.e., retain $u=\frac{1}{4}$ and $\eta=1$). This step can be imagined as the average of the energy change in converting one A atom into B in a $(AC)_1(AC)_1$ unit cell and one B into A in a $(BC)_1(BC)_1$ unit cell, and entails an energy change

$$\Delta E_{CE} = E[(AC)_1(BC)_1,a_{eq},\eta=1,u=\tfrac{1}{4}] - E[AC,a_{eq}] - E[BC,a_{eq}] \ . \quad (12)$$

This quantity measures the energy associated with charge redistribution during formation of the (unrelaxed) superlattice, reflecting "charge exchange" (CE). Each C atom is now coordinated by two A and two B atoms at equal distances. Since this need not be an equilibrium geometry, in the final step (iii), the geometry is relaxed to accommodate, to the extent possible via η and u, distinct AC and BC bond lengths and ideal tetrahedral bonds. This structural relaxation (S) step permits a *reduction* in energy

$$\Delta E_S = E[(AC)_1(BC)_1,a_{eq},\eta_{eq},u_{eq}] - E[(AC)_1(BC)_1,a_{eq},\eta=1,u=\tfrac{1}{4}] \equiv \Delta E_{SR} + \Delta E_{res} \ . \quad (13)$$

The energy ΔE_S itself includes (i) strain relief (SR) ΔE_{SR} upon relaxing η and u without charge redistribution, and (ii) a "residual" chemical energy ΔE_{res} due to whatever additional charge rearrangements are facilitated by changing atomic coordinates during relaxation. The first two lines of Eq. (13) are directly computable by first-principles calculations; the decomposition in the last line represents derived terms which provide physical insight and chemical trends. Within the valence-force-field description we use to evaluate ΔE_{SR} for $(AC)_1(BC)_1$, A—C and B—C bond parameters are "frozen" at their binary values. Labeling by FE such a "frozen-electron" VFF calculation and using the definition of ΔE_S [Eq. (13)] in terms of first-principles [self-consistent (SC)] calculations, we may write

$$\Delta E_{SR} = E_{FE}[a_{eq},\eta_{eq},u_{eq}] - E_{FE}[a_{eq},\eta=1,u=\tfrac{1}{4}] \quad (14a)$$

and

$$\Delta E_{res} = \{E_{SC}[a_{eq},\eta_{eq},u_{eq}] - E_{FE}[a_{eq},\eta_{eq},u_{eq}]\} - \{E_{SC}[a_{eq},\eta=1,u=\tfrac{1}{4}] - E_{FE}[a_{eq},\eta=1,u=\tfrac{1}{4}]\} \ . \quad (14b)$$

Each term in curly brackets in Eq. (14b), since it represents an electronic relaxation energy for fixed

geometry, must be negative, but $\Delta E_{\rm res}$ may be negative or positive.[61] Collecting all terms in Eqs. (11)–(13), we may write

$$\Delta H^O(1,1)=(\Delta E_{\rm VD}+\Delta E_{\rm SR})+(\Delta E_{\rm CE}+\Delta E_{\rm res})$$
$$\equiv \Delta E_{\rm MS}+\Delta E_{\rm chem}\ , \quad (15)$$

where the terms in parentheses correspond to those identified on the right-hand side. The largely independent effects of the lattice-mismatch between *AC* and *BC* compounds [microscopic strain (MS)] and electronegativity-related charge transfer [chemical (chem)] have now been isolated in, respectively, the terms $\Delta E_{\rm MS}$ and $\Delta E_{\rm chem}$ above. Simple approximate expressions for the terms in Eq. (15) are given in Sec. VI.

B. Decomposed energies and charge densities within the conceptual model

1. Energies

We have calculated the terms of Eq. (15) as follows: $\Delta E_{\rm VD}$, $\Delta E_{\rm CE}$, and ΔE_S were each obtained directly from the defining equations [Eqs. (11)–(13)] using first-principles pseudopotential calculations with $a_{\rm GaAs}=5.517$ Å, $a_{\rm AlAs}=5.604$ Å (Table II), and $a_{\rm eq}\simeq(a_{\rm GaAs}+a_{\rm AlAs})/2=5.5604$ Å. ΔE_S is found at the equilibrium geometry $a_{\rm eq}=5.5605$ Å, $\eta=1.000$, and $u=0.246$ (predicted by VFF calculations with first-principles GaAs and AlAs bond lengths). We find per four atoms

$$\Delta E_{\rm VD}=+14.25\ \text{meV}\ ,$$
$$\Delta E_{\rm CE}=+10.71\ \text{meV}\ , \quad (16)$$
$$\Delta E_S=-3.62\ \text{meV}\ .$$

(The LAPW value for $\Delta E_{\rm CE}$ is 11.3 meV.) The VFF calculations also predict $\Delta E_{\rm SR}$, the strain energy relieved upon relaxation from $(\eta=1,\ u=0.25)$ to $(\eta_{\rm eq},u_{\rm eq})$ without charge transfer (since binary elastic constants are used in VFF); $\Delta E_{\rm res}$ is by definition [Eq. (13)] $\Delta E_S-\Delta E_{\rm SR}$. We find

$$\Delta E_{\rm SR}=-7.80\ \text{meV}\ ,$$
$$\Delta E_{\rm res}=+4.18\ \text{meV}\ . \quad (17)$$

These results show the following.

(i) The superlattice is unstable relative to its constituents $[\Delta H^O(1,1)>0]$ since the positive net strain energy $\Delta E_{\rm MS}=+6.45$ meV is not compensated by a negative chemical energy: $\Delta E_{\rm chem}=+14.89$ meV. In contrast, compound-forming semiconductor alloys [e.g.,[19,20] Si $+C\rightarrow SiC$, or[21] ferromagnetic $CdTe+MnTe\rightarrow (CdTe)_1(MnTe)_1$] show a negative $\Delta E_{\rm chem}$ larger in magnitude than $\Delta E_{\rm MS}$.

(ii) $\Delta E_{\rm MS}$ is likely overestimated within the local-density calculations presented here: The relatively large theoretical lattice mismatch Δa between GaAs and AlAs means that excess strain is "frozen into" $(GaAs)_1(AlAs)_1$, GaAs, and AlAs at $a_{\rm eq}$. Simulating the very small experimental Δa by setting $\Delta E_{\rm MS}\simeq 0$, we still find $\Delta H^O(1,1)\simeq\Delta E_{\rm chem}=+14.89$ meV >0. We note that this value is very close to that of Bylander and Kleinman,[32] who found $\Delta a\simeq 0$ but $\Delta H^O(1,1)\simeq 15.5$ meV.

(iii) The chemical contributions $\Delta E_{\rm CE}=10.71$ meV and $\Delta E_{\rm res}=4.18$ meV are of the same sign and *add*, whereas the microscopic strain contributions $\Delta E_{\rm VD}$ and $\Delta E_{\rm SR}$ largely *cancel*. It is hence obvious that the instability of $(GaAs)_1(AlAs)_1$ is *chemical* in origin.

2. Charge densities

To understand the microscopic origins of this instability we examine the valence charge redistributions associated with each step described above, defined in analogy with Eqs. (11)–(13) above. In Fig. 3(a) we show the charge redistribution $\Delta\rho_{\rm VD}$ along bonds for GaAs (in the upper half frame) and for AlAs (in the lower frame). Dilation (compression) of GaAs (AlAs) to $a_{\rm eq}\simeq\bar{a}$ has essentially equal and opposite effects on the two constituents. As the Ga—As length increases, overlap between atoms is reduced, inducing a flow of valence charge from the bond back onto the atoms; for AlAs the bond length is reduced, permitting charge to flow onto the Al—As bond.[62] This distortion of equilibrium structures costs $\Delta E_{\rm VD}=+14.25$ meV.

In Fig. 3(b) we show $\Delta\rho_{\rm CE}$ (solid line) as the difference between densities along Ga—As and Al—As bonds in the unrelaxed superlattice and along the corresponding bonds in the zinc-blende materials, all at the same lattice constant. (The interfacial As atom experiences a different environment in the two zinc-blende phases, hence the discontinuity in $\Delta\rho_{\rm CE}$ there.) Charge is deposited on the Al—As bond at the expense of the Ga—As bond during this step, which is associated with a large positive change in energy ($\Delta E_{\rm CE}=+10.71$ meV).

Figure 3(b) shows (dashed line) $\Delta\rho_S$, the charge redistribution upon relaxing the superlattice. We note that, as in[25] $(GaP)_1(InP)_1$, relaxation *reverses* the direction of charge transfer with respect to the CE step given above. Failure to relax the superlattice in the presence of a substantial Δa could therefore lead to incorrect conclusions about the direction of net charge transfer in the superlattice. Similarly, we conclude that, when performing first-principles calculations for a superlattice, it is important to know the *theoretical* equilibrium bond lengths of the constituents (and not to simply take superlattice

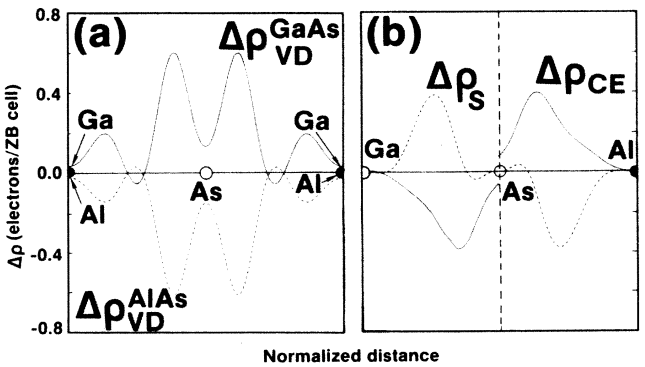

FIG. 3. Valence-charge-density redistribution along bonds associated with physical decomposition of superlattice formation into (a) volume deformation (VD), (b) charge exchange (CE), and (c) structural relaxation (*S*).

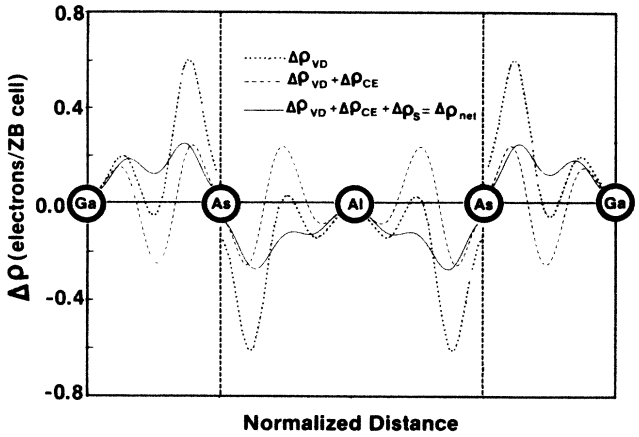

FIG. 4. Net charge density redistribution (with respect to equilibrium binary compounds) along bonds after volume deformation (VD, dotted line), charge exchange (VD + CE, dashed line), and net (VD + CE + S, solid line).

bond lengths to be the experimental values[63]) in order to determine delicate charge transfer effects.

In Fig. 4 we show charge density redistributions measured with respect to the *equilibrium* cubic compounds prevailing *after* each of the steps given above: $\Delta\rho_{\rm VD}$ [dotted line, repeated for completeness from Fig. 3(a)], $\Delta\rho_{\rm VD}+\Delta\rho_{\rm CE}$ (dashed line), and the net $\Delta\rho=\Delta\rho_{\rm VD}+\Delta\rho_{\rm CE}+\Delta\rho_S$. Comparing the charge density of $(GaAs)_1(AlAs)_1$ to those of GaAs and AlAs *where all three systems are kept at the same lattice constant* (i.e., $\Delta\rho_{\rm VD}+\Delta\rho_{\rm CE}$) we find *excess* density along the superlattice Al—As bond and a *deficit* of charge along the superlattice Ga—As bond. (However, *away* from the bond direction, an opposite trend exists.) This agrees with predictions of other calculations which maintain a fixed lattice, e.g., Massidda *et al.*[63] (who used the experimental lattice constants). The electrostatic origin of the driving force for relaxation of the anion displacement parameter u is apparent from this charge rearrangement $\Delta\rho_{\rm VD}+\Delta\rho_{\rm CE}$: The net deficit of electronic charge along the unrelaxed Ga—As bond (and corresponding excess along the Al—As bond) causes a distortion of the As anion toward Ga and away from Al, permitting each bond length to approach its equilibrium value.[62] The net result of superlattice formation (solid line) is an accumulation of charge on the Ga—As bond and a depletion on the Al—As bond by roughly the same magnitude. This transfer of charge from a *more stable* to a *less stable* bond (see cohesive energies in Table II) is the proximate cause for the instability of $(GaAs)_1(AlAs)_1$. This charge flow is in accord with the more attractive $l=0$ pseudopotential of Ga with respect to Al (Fig. 2) and the more negative s orbital energy of Ga relative to Al (Table I). It also agrees with a very recent measurement[64] of the Al nuclear magnetic resonance chemical shift in $Al_xGa_{1-x}As$ disordered alloys, which indicates charge transfer from the Al site to Ga as Ga content is increased. Our results for the *fully relaxed* charge density rearrangement $\Delta\rho$ differ from the recent prediction of Batra *et al.*,[33] which found an opposite charge transfer, with Pickett *et al.*[65] using empirical pseudopotentials [who found charge transfer for the (110) GaAs/AlAs interface to be negligible], and with Caruthers and Lin-Chung,[66] who found no charge transfer for (001) $(GaAs)_1(AlAs)_1$ using the empirical pseudopotential method.

Pietsch[67] recently used a simple model of overlapping two-electron molecules to simulate cubic GaAs and AlAs and Ga_2Al_2As clusters in a chalcopyrite structure (with a nearest-neighbor environment identical to that in the CuAu-I-like structure used in our calculations and observed by Kuan *et al.*[3]). He then extracted effective site and bond charges including electronegativity- and strain-induced charge transfer. He found, as we do, charge transfer from the AlAs to the GaAs bond; his results suggest that reduction of bonding charge is mostly associated with structural effects, while cation charges are mostly determined by electronegativity differences.

C. Fourier decomposition of superlattice charge density

The proximity to 1 of the equilibrium tetragonal distortion parameter η for $(GaAs)_1(AlAs)_1$ (Table III) makes possible an interesting decomposition of the Fourier components of ground-state properties (e.g., the

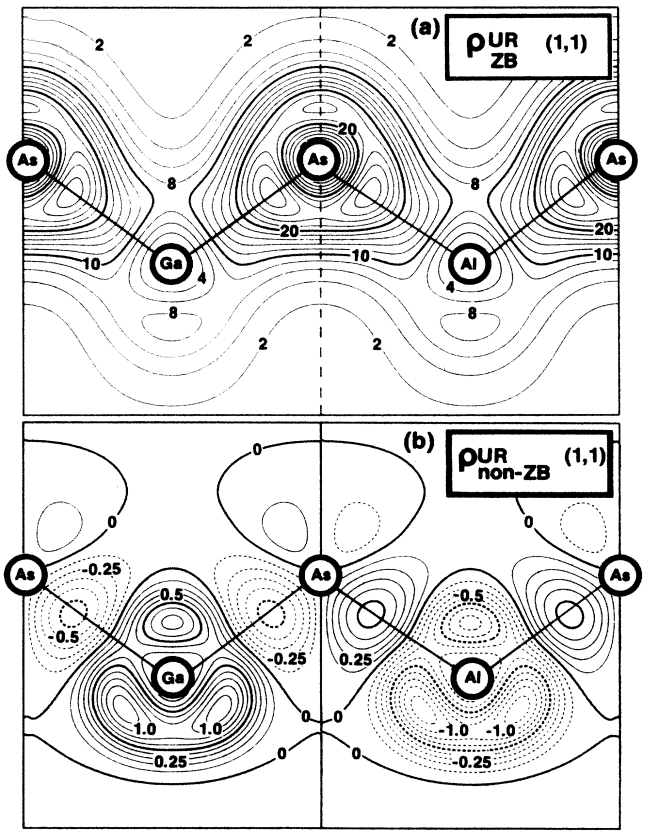

FIG. 5. Decomposition of ground-state valence charge density at $\bar{a}=5.560$ Å for unrelaxed [UR, $\eta=1$, $u=\frac{1}{4}$] $(GaAs)_1(AlAs)_1$ into (a) zinc-blende-like (ZB) and (b) strictly superlattice (non-ZB) contributions.

valence charge density or the crystal pseudopotential). For $\eta \simeq 1$ the reciprocal lattice consists of vectors $\mathbf{G}_{ZB}$ present for an fcc real-space lattice (e.g., GaAs or AlAs), responsible for the dominant features of the x-ray diffraction pattern, and the remainder, denoted $\mathbf{G}_{\text{non-ZB}}$, unique to the superlattice geometry and giving rise to the diffraction signature ("satellite spots") of the superlattice. In Fig. 5 this decomposition is shown pictorially at $a = \bar{a}$ for the unrelaxed (UR) lattice ($\eta = 1$ and $u = \frac{1}{4}$) in a $[0\,\bar{1}\,\bar{1}]$ plane through the interface. As expected, ρ_{ZB}^{UR} [Fig. 5(a)] does not distinguish between Ga and Al—it is virtually indistinguishable from the self-consistent charge density for the hypothetical $Ga_{0.5}Al_{0.5}As$ virtual-crystal zinc-blende structure at the same lattice constant. However, $\rho_{\text{non-ZB}}^{UR}$ [Fig. 5(b)] exhibits perfect antisymmetry with respect to interchange of Ga and Al. The non-ZB potential is responsible for depositing charge on the Ga site at the expense of the Al site and for augmenting the Al—As bond charge at the expense of the Ga—As bond charge. In Fig. 6(a) we show ρ_{ZB}^{RL} and $\rho_{\text{non-ZB}}^{RL}$ plotted along bonds for relaxed (RL) $(GaAs)_1(AlAs)_1$ using a common scale, emphasizing the small magnitude ($\sim 4\%$) of the non-ZB components. Relaxation [Fig. 6(b), solid line] accentuates the size of $\rho_{\text{non-ZB}}$ [with respect to the unrelaxed $\rho_{\text{non-ZB}}$, Fig. 6(b), dashed line] as the Ga—As and Al—As bonds are made more unlike, while leaving the Ga and Al sites unchanged. This also agrees with analysis of Pietsch[67] described above.

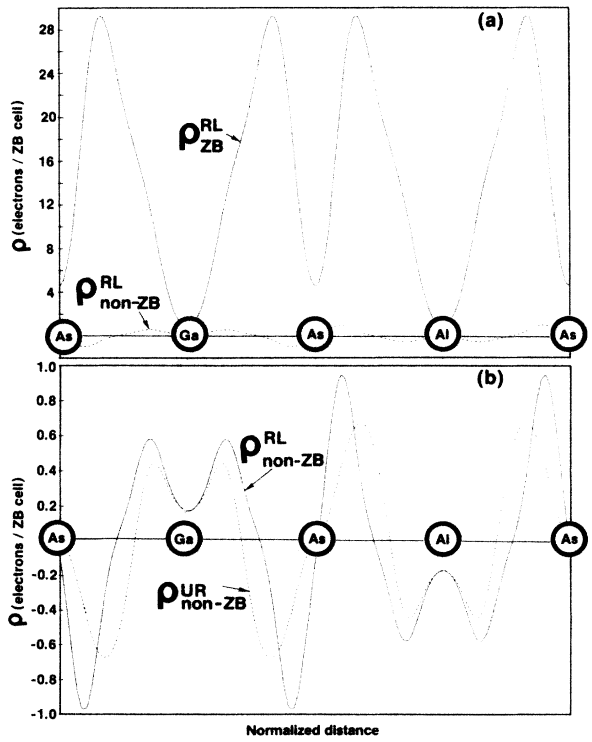

FIG. 6. (a) Zinc-blende-like (ZB) and non-ZB ground-state valence charge densities along bonds in relaxed (RL) $(GaAs)_1(AlAs)_1$; (b) non-ZB component for relaxed (RL, solid line) and unrelaxed (UR, dashed line) $(GaAs)_1(AlAs)_1$ at $a = \bar{a}$.

VI. SIMPLE MODEL FOR FORMATION ENTHALPY OF [001] $(AC)_1(BC)_1$

In this section we develop simple analytic expressions for the dominant contributions ΔE_{VD}, ΔE_{CE}, and ΔE_{SR} to the net formation enthalpy $\Delta H^O(1,1)$ of the perfectly ordered $(AC)_1(BC)_1$ [001]-orientation superlattice. These expressions can be used to assess trends in stability energies.

A. Elastic energies

Using observations based on valence-force-field calculations, useful closed-form approximations may be derived for the elastic contributions ΔE_{VD} and ΔE_{SR} [Eqs. (11) and (14a)] to the superlattice formation enthalpy. In the harmonic regime all strain energies vary quadratically about their equilibrium (eq) values. For a pure cubic binary phase with two atoms per primitive cell (of volume $V = a^3/4$ for a fcc Bravais lattice) we find

$$E(a) \simeq E(a_{eq}) + \tfrac{1}{2}(d^2E/dV^2)_{eq}(V - V_{eq})^2$$
$$\simeq E(a_{eq}) + \tfrac{9}{8}Ba_{eq}(a - a_{eq})^2 \qquad (18)$$

per primitive cell, where B is the cubic material bulk modulus. The zinc-blende structure is perfectly strain-free at the equilibrium lattice parameter, hence for it $E(a_{eq}) = 0$. Grown epitaxially, the cubic material tetragonally distorts so that for every value of $a_{\parallel} = a_s$ (Sec. II) the tetragonal dimension c minimizes the elastic energy density. Under these conditions one finds (Appendix A and Ref. 40) the same form as Eq. (18) but with B replaced by B^*, where for the [001] orientation $B^*/B = \frac{2}{3}(1 - C_{12}/C_{11})$. Typically for III-V zinc-blende semiconductors $B/B^* \simeq 2.5$–3. Using Eq. (18), we find that ΔE_{VD} of Eq. (11) for $a_{eq} \simeq \bar{a} = \frac{1}{2}(a_{AC} + a_{BC})$ is

$$\Delta E_{VD} \simeq \tfrac{9}{16}\bar{B}\bar{a}(\Delta a)^2 , \qquad (19)$$

where $\bar{B}$ is the average cubic bulk modulus and

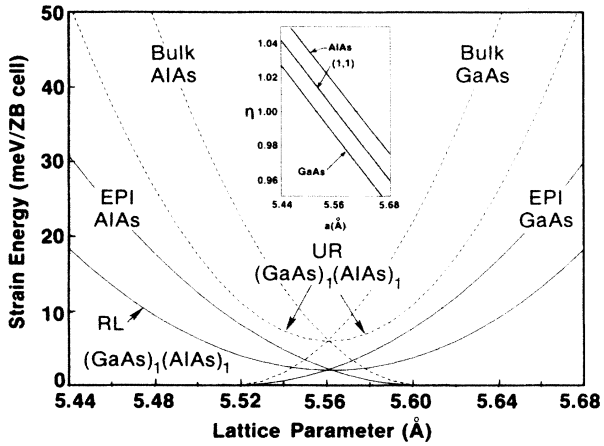

FIG. 7. Strain energies within VFF description for cubic GaAs and AlAs and unrelaxed $(GaAs)_1(AlAs)_1$ (UR, $\eta \neq 1$, $u \neq \frac{1}{4}$), dashed lines, and epitaxial (epi) GaAs and AlAs and fully relaxed (RL, η_{eq}, u_{eq}) $(GaAs)_1(AlAs)_1$.

$\Delta a = a_{AC} - a_{BC}$.

To estimate ΔE_{SR} we note that within our VFF strain only calculations

$$E[(AC)_1(BC)_1, a_s, \eta_{eq}, u_{eq}] - E[AC, a_s] - E[BC, a_s] \simeq 0$$

for all a_s and

$$E[(AC)_1(BC)_1, a, \eta = 1, u = \tfrac{1}{4}] \simeq E[AC, a] + E[BC, a]$$

for all a [see Fig. 7, Appendix A, and Fig. 3 in Ref. 40(b)]. We can thus express the strain energy for the (unrelaxed or relaxed) ternary as a sum of those for the (cubic or tetragonally-distorted) binaries (characterized respectively by B and B^*) at $a_{eq} \simeq \bar{a}$. Since the strain relief energy ΔE_{SR} is given by Eq. (14a) and $a_{eq} \simeq \bar{a}$, we find

$$\Delta E_{SR} \simeq \tfrac{9}{16} \bar{a} (\Delta a)^2 (\bar{B}^* - \bar{B}) \tag{20}$$

with $\bar{B}^*$ the average of the binary elastic moduli B^* and $\bar{B}$ the average binary bulk modulus. Since we expect $\bar{B}/\bar{B}^*$ to be ~ 2.5–3, ΔE_{SR} is negative; relaxation reduces the strain in the superlattice by 60–70%. Note that $\Delta E_{MS} = \Delta E_{VD} + \Delta E_{SR}$ does not depend on $\bar{B}$ and is positive definite:

$$\Delta E_{MS} \simeq \tfrac{9}{16} \bar{a} \bar{B}^* (\Delta a)^2 , \tag{21a}$$

$$B^* = \tfrac{2}{3} B (1 - C_{12}/C_{11}) . \tag{21b}$$

B. Chemical energies: Ordered superlattice versus disordered alloy

We model ΔE_{CE} for both the superlattice and the disordered alloy using a simple electrostatic energy approach including both interatomic (Madelung energy, "Madelung") and intra-atomic (on-site "OS") Coulomb effects. We will take $\eta = 1$ and $u = \frac{1}{4}$ (hence, $R_{AC} = R_{BC} = R$) for convenience in describing the superlattice, and will assume A and B atoms to have nonoverlapping spherical charge distributions with charges Q_A and Q_B (and charge difference $\Delta Q = Q_A - Q_B$), respectively, in the $(AC)_1(BC)_1$ [001]-orientation superlattice, in general different[68] from their charges q_A and q_B (and difference $\Delta q = q_A - q_B$) in the isolated zinc-blende compounds AC and BC. We assume the anions C have the charge needed to neutralize their A and B nearest neighbors and, for conservation of cation charge, $Q_A + Q_B = q_A + q_B$. [Indeed, we find the net LAPW charge on the anion sublattice to be approximately constant in forming $(AC)_1(BC)_1$ from AC and BC.] Any interatomic charge transfer must occur at the expense of depletion or addition of on-site atomic charge. Following van Schilfgaarde *et al.*,[69] we take the dependence of the electrostatic energy of atom type α on its net charge q to be

$$E_\alpha(q) \simeq E_\alpha(0) - \varepsilon_\alpha q + \tfrac{1}{2} U_\alpha q^2 + \cdots ,$$

where $E_\alpha(0)$ is the total energy of the neutral atom, ε_α is the single-particle eigenvalue of the highest occupied valence orbital, and U_α is the Mott-Hubbard Coulomb energy. Combining interatomic and intra-atomic Coulomb effects, we may write for either the ordered (O) superlattice or the disordered (D) alloy

$$\Delta E_{CE} \simeq \Delta E_{Madelung} + \Delta E_{OS} , \tag{22}$$

where the excess Madelung energy of the ordered structure is found to be (per four atoms)

$$\begin{aligned} \Delta E^O_{Madelung}(1,1) \equiv & E_{Madelung}[(AC)_1(BC)_1] \\ & - E_{Madelung}[AC] - E_{Madelung}[BC] \\ = & [(\Delta q)^2/R] \\ & \times [\alpha^{ZB}/2 - (\sqrt{6}/16)\alpha^{(1,1)}(\Delta Q/\Delta q)^2], \end{aligned} \tag{23}$$

and the excess on-site Coulomb energy (for convenience taking[70] $\Delta Q/\Delta q = 1$; see Appendix B) is (per four atoms)

$$\begin{aligned} \Delta E^O_{OS}(1,1) \equiv & E^O_{OS}[(AC)_1(BC)_1] - E_{OS}[AC] - E_{OS}[BC] \\ = & -U_C(\Delta Q)^2/4 . \end{aligned} \tag{24}$$

In Eq. (23), $\alpha^{ZB} = 1.638\,055$ and $\alpha^{(1,1)} = 1.594\,367$ are Madelung constants for the zinc-blende structure and the cation sublattice in ABC_2, respectively. It is obvious that in order for $\Delta E^O_{Madelung}(1,1)$ to be negative, formation of the superlattice must *amplify*[68] the relative cation charge disparity $\Delta Q/\Delta q$ by a factor of at least $(8\alpha^{ZB}/\sqrt{6}\alpha^{(1,1)})^{1/2} = 1.83$. In contrast, $\Delta E^O_{OS}(1,1)$ favors compound formation (i.e., is negative) for all $\Delta Q \neq 0$.

Equations exactly analogous to Eqs. (23) and (24) may be written for the *random* alloy (see Appendix B). We find[71]

$$\Delta E^D_{Madelung}(x) = 3\,\Delta E^O_{Madelung}(1,1) x(1-x) \tag{25}$$

for[70] any value of the ratio $\Delta Q/\Delta q$, and

$$\Delta E^D_{OS}(x) = 3\,\Delta E^O_{OS}(1,1) x(1-x) \tag{26}$$

for $\Delta Q/\Delta q = 1$. This shows that for $x = 0.5$,

$$\Delta E^D_{CE} = \tfrac{3}{4}\,\Delta E^O_{CE} , \tag{27a}$$

and for the case $\Delta Q = \Delta q$, per four atoms,

$$\Delta E^D_{CE} \simeq \tfrac{3}{4}(\Delta Q)^2 \left[\frac{0.5749}{R} - U_C/4 \right] . \tag{27b}$$

The *relative* excess Madelung energies of the ordered superlattice and the disordered alloy of the same composition obviously depend on the ratio $\Delta Q/\Delta q$: if $\Delta E^O_{Madelung}(1,1) < 0$, the ordered phase $A_n B_{4-n} C_4$ is more stable than the disordered phase for any $x = x_n = n/4$. If $\Delta E^O_{Madelung}(1,1) > 0$ [as we find below for $(GaAs)_1(AlAs)_1$], the Madelung formation energy of the *random* alloy lies *below* than for the ordered phase. In contrast, the on-site Coulomb term stabilizes the ordered phase over the disordered phase for all $\Delta Q = \Delta q \neq 0$.

van Schilfgaarde *et al.*[69] calculated $\Delta E^D_{Madelung}$, incorrectly omitting a factor of $\frac{1}{2}$ in one of their Madelung

terms[72] for the disordered phase (see Appendix B). They erroneously predicted[69] a substantial *stabilization* of $\Delta E^O_{\text{Madelung}}+\Delta E^O_{\text{OS}}$ over $\Delta E^D_{\text{Madelung}}+\Delta E^D_{\text{OS}}$. Using their values for GaAs/AlAs, i.e., $U_C=9.49$ eV, $\Delta Q/2\simeq 0.02e$, and the experimental average GaAs/AlAs bond length [but with the corrected expression,[69] or Eq. (25)] shows the random alloy to have an energy comparable (within a fraction of a meV) to that of the ordered superlattice, including both Madelung and on-site terms. Since the formation energy for either phase is positive, each is unstable with respect to decomposition into the zinc-blende constituents. This simple estimate shows that, due to the effective cancellation between on-site and long-range Coulomb effects, the electrostatic energy does not distinguish the ordered superlattice from the disordered alloy (in contrast with the conclusion of Ref. 69) unless strong charge transfer $(\Delta Q-\Delta q)$ occurs. The factor which *stabilizes* the ordered superlattice relative to the disordered alloy in lattice mismatched systems is the strain energy, since[25] $\Delta E^D_{\text{MS}}>\Delta E^O_{\text{MS}}$ for $|\Delta a|>0$.

C. Analytic expression for $(AC)_1(BC)_1$ formation enthalpy

Using the results of the previous two sections, we may now estimate the total formation enthalpy of [001]-orientation $(AC)_1(BC)_1$ from simple model calculations, and compare them with the results of first-principles calculations. Neglecting the relatively small term ΔE_{res}, we may write the components of $\Delta H^O(1,1)=\Delta E^O_{\text{MS}}+\Delta E^O_{\text{CE}}$, using Eqs. (21), (23), and (24) as

$$\Delta E^O_{\text{MS}}=\Delta E^O_{\text{VD}}+\Delta E^O_{\text{SR}}\simeq 0.003\,511\bar{B}^*\bar{a}(\Delta a)^2\ , \tag{28}$$

$$\begin{aligned}\Delta E^O_{\text{CE}}&\simeq\Delta E^O_{\text{Madelung}}(1,1)+\Delta E^O_{\text{OS}}(1,1)\\&=27.24(\Delta q/e)^2[1-0.298(\Delta Q/\Delta q)^2]/\bar{a}\\&\quad-0.25U_C(\Delta Q/e)^2\end{aligned} \tag{29}$$

in eV per four atoms, where $\bar{a}=(a_{AC}+a_{BC})/2$ and $\Delta a=a_{BC}-a_{AC}$ are in Å, the average binary elastic modulus $\bar{B}^*$ is in GPa [Eq. (21b)], and U_C is the anion (atom C) Coulomb integral in eV. Here we have taken, in accord with the results of Sec. IV, the equilibrium lattice constant of the superlattice to be $\bar{a}$, the average of those of its zinc-blende constituents.

We can evaluate the elastic energy terms of Eqs. (19)–(21) by taking $B^*(\text{GaAs})=28.09$ GPa and $B^*(\text{AlAs})=29.89$ GPa from our VFF results [or, using Eq. (21b), $B^*(\text{GaAs})=28.1$ GPa and $B^*(\text{AlAs})=29.5$ GPa], and $a=5.560$ Å from Table II. Using the theoretical (exaggerated) $\Delta a=0.087$ Å from Table II, we find per four atoms

$$\begin{aligned}\Delta E_{\text{VD}}&=+12.1\text{ meV}\ ,\\ \Delta E_{\text{SR}}&=-7.8\text{ meV}\ ,\\ \Delta E_{\text{MS}}&=+4.3\text{ meV}\ .\end{aligned} \tag{30}$$

The similarity of these results to those calculated from the first-principles total energies [Eqs. (16)–(17)] supports the model we use. Clearly, using the *experimental* $\Delta a\lesssim 0.01$ Å one finds $\Delta E_{\text{MS}}\simeq 0$.

$\Delta E^O_{\text{Madelung}}$ can be calculated using $R=(\sqrt{3}/4)\bar{a}=2.45$ Å and $\Delta q=+0.07e$, $\Delta Q=+0.06e$ (obtained by integrating the charges within the muffin-tin spheres in the LAPW calculation). ΔE^O_{OS} is estimated using the atomic value[69] $U_{\text{As}}=9.49$ eV and the estimated average[69] $\Delta Q=\Delta q\simeq 0.04e$. This yields

$$\begin{aligned}\Delta E^O_{\text{Madelung}}&\simeq 21\text{ meV}\ ,\\ \Delta E^O_{\text{OS}}&\simeq -3.8\text{ meV}\ ,\\ \Delta E^O_{\text{CE}}&\simeq 17.2\text{ meV}\ ,\end{aligned} \tag{31}$$

compared with $\Delta E^O_{\text{CE}}\simeq 10.71$ meV [Eq. (16)] obtained by direct pseudopotential total-energy calculations or with $\Delta E_{\text{CE}}=11.3$ meV obtained as the chemical energy in the LAPW calculation.

Equations (28) and (29) explicitly display the competition between destabilizing lattice mismatch effects and potentially stabilizing charge-transfer effects (provided $\Delta Q/\Delta q$ is sufficient). The expectation that charge transfer will be correlated with electronegativity differences $\Delta\chi=\chi_A-\chi_B$ suggests that superlattices $(AC)_1(BC)_1$ with large $\Delta\chi$ are more likely to be stabilized by ΔE_{chem}. However, orbital radii analyses suggest that a large $\Delta\chi$ is often associated with substantial Δa. Hence rigorous predictions on stability trends appear difficult to make, since charge transfer and strain effects have competing yet correlated effects.

VII. ELECTRONIC STRUCTURE OF $(\text{GaAs})_1(\text{AlAs})_1$

The electronic structure of an ordered compound may be radically different from that of its constituents, leading to possible direct-gap ordered compounds derived from indirect-gap components.[73,74] Considerable theoretical attention has recently been given[75–78] to the electronic band structure of $(\text{GaAs})_m(\text{AlAs})_m$. For thick superlattices, Kronig-Penney-type models are quite satisfactory in interpreting experimentally-observed electronic properties of these systems.[1] Such models are based on the assumption of a transition between material properties characteristic of AC and those of BC which is abrupt on the scale of the quantum-well-layer thickness. For small (m,m), however, the scale of variation of the electronic potential is an appreciable fraction of the layer thickness, and microscopic calculations are required to understand electronic properties. We will examine how the electronic structure of $(\text{GaAs})_1(\text{AlAs})_1$ is related to those of GaAs and AlAs in three steps: (i) form a $Ga_{0.5}Al_{0.5}As$ zinc-blende (fcc) random alloy and model its properties by the VCA; (ii) fold the VCA bands into the smaller Brillouin zone appropriate to the doubled unit cell of the ordered $(\text{GaAs})_1(\text{AlAs})_1$ superlattice, and (iii) switch on the ordering potential $V_{\text{ord}}\equiv V[(\text{GaAs})_1(\text{AlAs})_1]-V_{\text{VCA}}$ which carries the VCA alloy into the ordered superlattice.

(i) *VCA step.* In comparing the electronic structure of the equilibrium VCA $Ga_{0.5}Al_{0.5}As$ alloy with those of their constituents at their equilibria, there are two

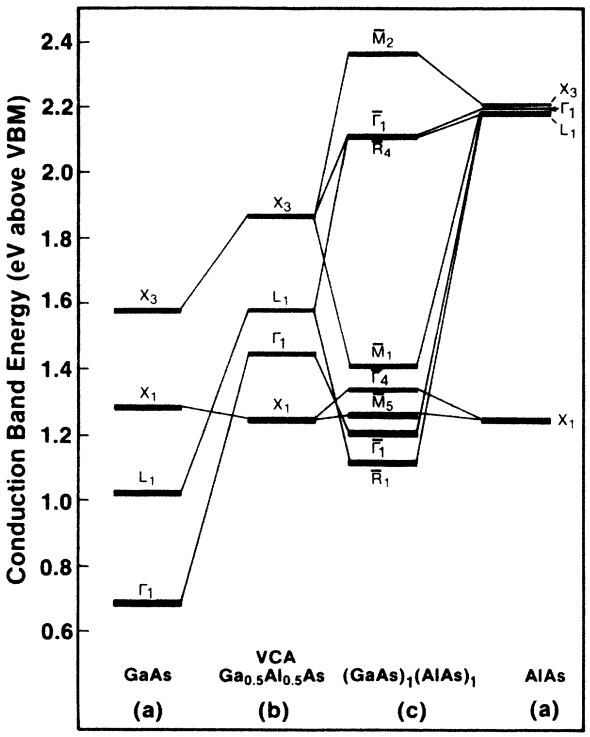

FIG. 8. Conduction-band eigenvalues at Γ, L, and X points of the face-centered-cubic Brillouin zone at $a=5.56$ Å for GaAs, AlAs, fictitious $Ga_{0.5}Al_{0.5}As$ VCA alloy, and unrelaxed $(GaAs)_1(AlAs)_1$.

effects: (a) deformation potential-induced[79] shifts in the constituents as GaAs (AlAs) is dilated (compressed) to $\bar{a}$ and (b) averaging the states of AC and BC both at $\bar{a}$ (the dominant contribution). We show in Fig. 8 conduction bands for GaAs and AlAs [Fig. 8(a)], and the VCA $Ga_{0.5}Al_{0.5}As$ alloy [Fig. 8(b)] at high-symmetry points of the fcc Brillouin zone, all calculated self-consistently at the average theoretical lattice constant, $\bar{a}=5.56$ Å. We find that the VCA conduction bands at Γ, X, and L all fall below the average of those GaAs and AlAs (at $\bar{a}$ or their respective equilibrium a), and that the VCA compound is an indirect-gap material at X_{1c}, both observations in qualitative agreement with experimental data.[80-83] The VCA optical bowing coefficient b for a band eigenvalue ε of $Ga_xAl_{1-x}As$ is defined by

$$\varepsilon_{\rm VCA}=x\varepsilon_{AC}+(1-x)\varepsilon_{BC}-bx(1-x)\ .$$

These are given in Table IV, together with the experimental values,[81-83] and other calculations.[84] Clearly, the VCA underestimates the bowing.

(ii) *Band-folding step.* Each point in the smaller tetragonal Brillouin zone (BZ) of the superlattice corresponds[32,85,86] to two distinct fcc BZ points; we label superlattice points with an overbar. The folding relations are $\Gamma_{1c}\leftrightarrow\bar{\Gamma}_{1c}$, $X_{1c}\leftrightarrow\bar{\Gamma}_{4c}+\bar{M}_{5c}$, $X_{3c}\leftrightarrow\bar{\Gamma}_{1c}+\bar{M}_{1c}+\bar{M}_{2c}$, and $L_{1c}\leftrightarrow\bar{R}_{1c}+\bar{R}_{4c}$. Folding hence produces extra degeneracies at $\bar{M}$ and $\bar{R}$ without shifting the band energies relative to the VCA. It also produces two new pseudodirect states $\bar{\Gamma}_4(X_{1c})$ and $\bar{\Gamma}_1(X_{3c})$, where we indicate in parentheses the fcc states which are folded in.

(iii) *Ordering step.* Finally, the ordering potential $V_{\rm ord}$ shown in Fig. 9(a) will (a) lift the degeneracy between states whose spatial distribution is along or perpendicular to the superlattice stacking direction, and (b) split states with cation s character into a lower GaAs-like and an upper AlAs-like state, reflecting the more attractive Ga $l=0$ pseudopotential (see Fig. 2). States with no s character about the cation sites are only weakly split by $V_{\rm ord}$ since the $l=1$ pseudopotential of Al is only slightly more attractive than that of Ga. $V_{\rm ord}$ will lead to a repulsion between states of the same symmetry, e.g., $\bar{\Gamma}_{1c}(X_{3c})$ and $\bar{\Gamma}_{1c}(\Gamma_{1c})$, and is also responsible for the redistribution of valence charge density [Fig. 9(b)] with respect to the VCA that gives rise to superlattice spots in the x-ray diffraction pattern.

Figure 8(c) shows the way band eigenvalues of the tetragonal BZ for unrelaxed $(GaAs)_1(AlAs)_1$ evolve from those of GaAs, AlAs, and the VCA $Ga_{0.5}Al_{0.5}As$ alloy all at $\bar{a}$. [The superlattice eigenvalues shown change by less than 0.01 eV upon relaxation of the structural parameters η and u; the only exception—labeled $\bar{\Gamma}_4$—is the quantum confined state described below.] The lowest conduction band at the X point of the VCA alloy, X_{1c}, derives from the corresponding GaAs and AlAs X_{1c} points. Having chosen the origin at the anion site, X_{1c} has sd character on the anion and pd character on the cation, while the reverse is true for X_{3c}. Because of the great similarity of the $l=1$ pseudopotentials for Ga and Al (Fig. 2), the X_{1c} states for GaAs, AlAs, and the VCA alloy are close. In going to the superlattice [Figs. 10(a)-10(c)] the VCA X_{1c} state splits into a lower

TABLE IV. Bowing parameters, in eV, for the $Ga_xAl_{1-x}As$ alloy and the ordered $GaAlAs_2$ compound. PS denotes pseudopotential; LAPW, linearized augmented plane wave; TB, tight binding; CPA, coherent potential approximation.

	Disordered alloy				Ordered $GaAlAs_2$ ($b_{\rm ord}$)		
	VCA (PS)	VCA TB[a]	CPA TB[a]	Expt.	Present (PS)	Present (LAPW)	Ref. 32
$b(\Gamma_{1c})$	0.00	0.03	0.16	0.37[b]	0.97	0.78	0.74
$b(X_{1c})$	0.06	0.00	0.12	0.15[c]-0.245[b]	0.01	0.05	-0.05[d]
$b(L_{1c})$	0.08	0.01	0.14	0.055[b]	1.90	2.10	1.81

[a]Reference 84.
[b]Reference 81.
[c]References 82 and 83.
[d]$b[\bar{\Gamma}_4(X_{1c})]=-0.08$ (PS, present).

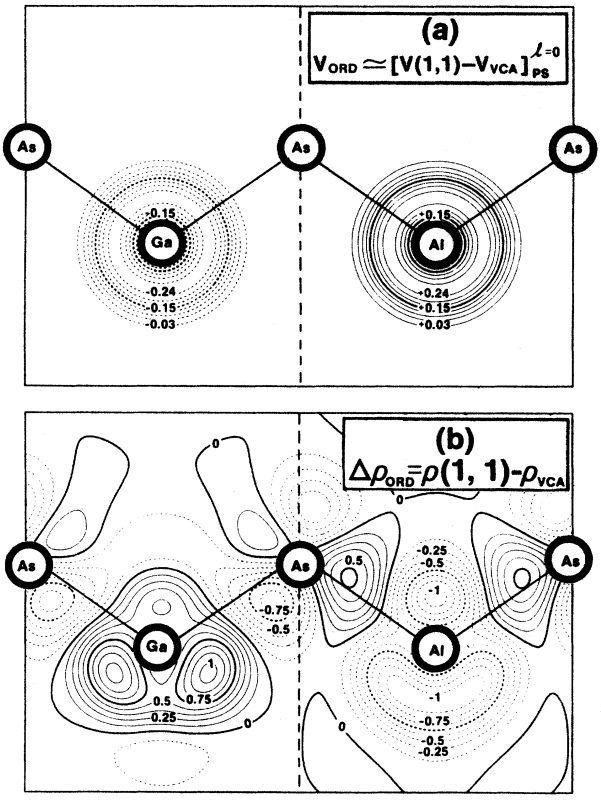

FIG. 9. (a) Perturbation in potential in Ry, and (b) the density response it induces (in electrons per zinc-blende cell), due to ordering of the VCA alloy.

doubly-degenerate $\bar{M}_{5c}$ state [Fig. 10(b), composed of Ga and Al p_x and p_y orbitals] and an upper singly degenerate state $\bar{\Gamma}_{4c}$ [Fig. 10(c), composed of Ga and Al p_z orbitals]. As perturbation theory would suggest, the $\bar{M}_{5c}$ state has strong Ga and Al character with a slight excess of Al character because the AlAs X_{1c} state lies lower in energy, reflecting the slightly more attractive $l=1$ Al pseudopotential. The upper state $\bar{\Gamma}_{4c}$ [Fig. 10(c)] lies above either of the constituent X_{1c} points. Because of its strong anion character and the fact that the Ga and Al p_z orbitals sample the superlattice repeat distance, it is this state which is most sensitive to the Ga-As-Al interplanar spacings and the structural parameters u and η which control the anion position.

For the remaining VCA conduction bands shown in Fig. 10 the interpretation of the splitting of VCA states by the non-VCA components of the superlattice potential closely follows the relative amounts of cation s and p character of the VCA state: all are split into lower, GaAs-like, and upper, AlAs-like, states. The total pseudopotential splittings for the VCA conduction-band states $\Gamma_{1c}[\bar{\Gamma}_{1c}(X_{3c})-\bar{\Gamma}_{1c}(\Gamma_{1c})]$, $X_{3c}[\bar{M}_{2c}-\bar{M}_{1c}]$, and $L_{1c}[\bar{R}_{4c}-\bar{R}_{1c}]$ are 0.93, 0.96, and 0.99 eV, respectively (the corresponding LAPW figures are 1.14, 0.96, and 1.0 eV). [The symmetry-induced repulsion between states $\bar{\Gamma}_{1c}(X_{3c})$ and $\bar{\Gamma}_{1c}(\Gamma_{1c})$ is so strong that we describe them as a complementary pair: see Figs. 10(e)–10(f).] In the zinc-blende VCA alloy the Γ_{1c} state has cation s but not p character, and exhibits the usual antibonding s character; its splitting samples only the difference in Ga and Al $l=0$ pseudopotentials. The next-highest energy VCA state L_{1c} has both cation s and p character. Interestingly, the superlattice compatibility relations require this state to split into an $\bar{R}_{1c}$ state [consisting of Ga s and p_z orbitals and Al (p_x+p_y) orbitals] and a complementary $\bar{R}_{4c}$ state. This is evident in Figs. 10(g)–10(i); the splitting $|\varepsilon(\bar{R}_{4c})-\varepsilon(\bar{R}_{1c})|$ is the largest of all conduction bands shown because it samples the difference in both the s- and p-wave pseudopotentials for Ga and Al. One result of this amplification of cation difference is that *$(GaAs)_1(AlAs)_1$ is indirect by way of the $\bar{R}$ (L_{1c}) point* (whereas the VCA alloy is indirect via X_{1c}). Finally, the VCA X_{3c} state, with strong cation s character, is split [Figs. 10(j)–10(l)] into states $\bar{M}_{1c}$ and $\bar{M}_{2c}$ with cation-centered lobes.

The preceding discussion shows that the states of ordered $GaAlAs_2$ differ from those of the disordered $Ga_{0.5}Al_{0.5}As$ alloy. This can be quantified by defining "optical bowing parameters" for the *ordered* (ord) phase $GaAlAs_2$ as

$$\begin{aligned} b_{\rm ord}(\bar{\Gamma}_{1c}) &= 4[\bar{\varepsilon}(\Gamma_{1c})-\varepsilon(\bar{\Gamma}_{1c}(\Gamma_{1c}))] , \\ b_{\rm ord}(\bar{X}_{1c}) &= 4[\bar{\varepsilon}(X_{1c})-\varepsilon(\bar{M}_{5c}(X_{1c}))] , \\ b_{\rm ord}(\bar{L}_{1c}) &= 4[\bar{\varepsilon}(L_{1c})-\varepsilon(\bar{R}_{1c}(L_{1c}))] , \end{aligned} \tag{32}$$

where $\bar{\varepsilon}$ denotes the composition-weighted average of the corresponding zinc-blende gaps of GaAs and AlAs at their equilibrium lattice parameters. Table IV shows the bowing parameters for the ordered phase, where they are compared with those of the disordered alloy. Clearly the $\bar{\Gamma}_{1c}(\Gamma_{1c})$, $\bar{M}_{5c}(X_{1c})$, and $\bar{R}_{1c}(L_{1c})$ states of the ordered phase are substantially lower in energy than the corresponding VCA states of $Ga_{0.5}Al_{0.5}As$, leading to far larger bowing parameters in the ordered phase. This increase in bowing (reduction in gap) is the hallmark of ordering[85] of an alloy, and has been observed in $Ga_xIn_{1-x}P$ (Ref. 9) and $Ga_xIn_{1-x}As$ (Ref. 5).

Bernard and Zunger[86] have suggested that for alloys of constituents AC and BC which differ considerably in lattice parameter and electronegativities, the experimental alloy bowing $b_{\rm expt}$ cannot be described adequately by the VCA. In general, $b_{\rm expt}$ can be thought to consist of an "ordered" part $b_{\rm ord}$, calculable, e.g., from the properties of ABC_2, plus a disorder part $b_{\rm dis}$,

$$b_{\rm expt} = b_{\rm ord} + b_{\rm dis} . \tag{33}$$

The sum of $b_{\rm ord}$ and $b_{\rm dis}$ can be usefully approximated by considering an average alloy gap calculated from a weighted superposition of the band gaps of all local environments appearing in the alloy (see Appendix B). They reproduced the observed band gaps of zinc chalcogenides[86] and concluded that, while for alloys with lattice-matched constituents the disorder contribution $b_{\rm dis}$ can be large, for alloys of lattice mismatched constituents $|b_{\rm ord}| \gg |b_{\rm dis}|$, and hence $b_{\rm expt}$ could be modeled approximately by $b_{\rm ord}$. Here, our results (Table IV) for the lattice-matched system $Ga_xAl_{1-x}As$ indeed suggest that $b_{\rm dis} \simeq (b_{\rm expt}-b_{\rm ord})$ is large; in agreement

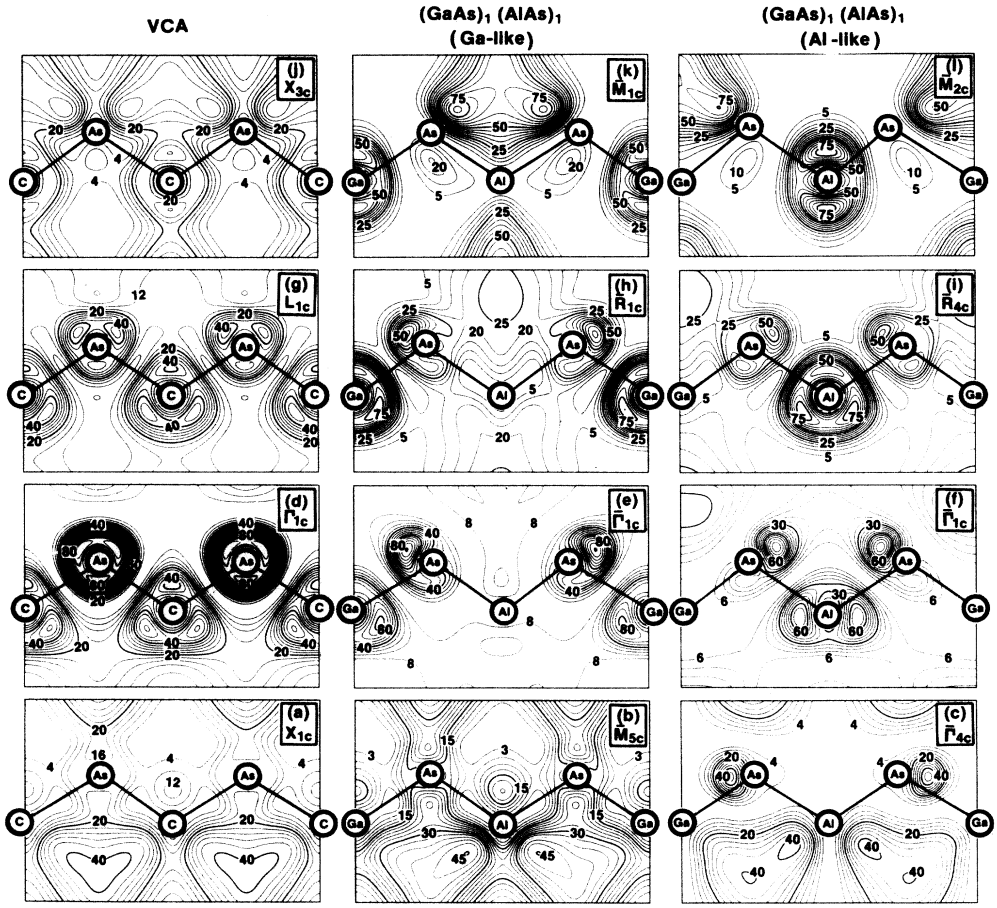

FIG. 10. Conduction-band wave-function amplitudes (in electrons per volume $a^3/4$) for unrelaxed $(GaAs)_1(AlAs)_1$ at $a=5.56$ Å at high-symmetry Brillouin-zone points. (e) and (f) derive, respectively, from zinc-blende Γ_{1c} and X_{3c} states.

with Ref. 86, disorder effects tend to *reduce* the magnitude of the bowing parameters deduced from the ordered phase.

VIII. COMPARISON OF CALCULATED ELECTRONIC STRUCTURE WITH EXPERIMENT

Recently, four experimental studies[87–90] of the spectra of ultrathin $(GaAs)_n$ $(AlAs)_n$ have appeared. We compare here our predictions with experiment and discuss some predicted, but so far unobserved, transitions. For comparison with experiment, theoretical superlattice band energies need to be corrected for LDA error. We note [Figs. 8 and 10] that $\bar{R}_{1c}$ and $\bar{M}_{1c}$ are GaAs L_{1c}- and X_{3c}-like, respectively, while $\bar{M}_{5c}$ and $\bar{\Gamma}_{4c}$ (both derived from X_{1c}) exhibit mixed GaAs and AlAs character with some emphasis on AlAs. $\bar{\Gamma}_{1c}(\Gamma_{1c})$ [Fig. 10(e)] we find to be predominantly GaAs Γ_{1c}-like. We may thus approximately correct for LDA errors by using the corresponding corrections for bulk GaAs at L_{1c} and X_{3c} (for $\bar{R}_{1c}$ and $\bar{M}_{1c}$), the averaged corrections for bulk GaAs and AlAs at X_{1c} (for $\bar{M}_{5c}$ and $\bar{\Gamma}_{4c}$) and for GaAs at Γ_{1c} (for $\bar{\Gamma}_{1c}$). This yields (using our relaxed LAPW results) corrections of 1.0, 1.29, 0.79, 0.79, and 0.76 eV for $\bar{R}_{1c}$, $\bar{\Gamma}_{1c}$, $\bar{M}_{5c}$, $\bar{\Gamma}_{4c}$, and $\bar{M}_{1c}$, respectively. The uncorrected LDA results (0.88, 0.85, 1.30, 1.41, and 1.31 eV, respectively) become, after correction, 1.88, 2.14, 2.09, 2.20, and 2.07 eV at $T=0$ K, all measured with respect to the valence-band maximum $E_{\rm VBM}$. (Although both LDA corrections and LDA band energies obtained with the pseudopotential method differ from LAPW results, the *corrected* transition energies are nearly identical for both methods.) Analogous corrections for the VCA alloy (using pseudopotential results) predict the states L_{1c} at 2.42 eV, Γ_{1c} at 2.24 eV, and X_{1c} at 2.10 eV, all with respect to $E_{\rm VBM}$.

Based on our corrected band energies for $(GaAs)_1(AlAs)_1$ we now discuss its spectrum, referring all state energies to $E_{\rm VBM}$.

(i) *Direct band gap.* We predict the $\bar{\Gamma}_v \rightarrow \bar{\Gamma}_{1c}(\Gamma_{1c})$ direct gap ("E_0 transition") at 2.14 eV, i.e., 0.10 eV below the calculated direct transition for the $Ga_{0.5}Al_{0.5}As$ disordered alloy and 0.185 eV below the average of the E_0 energies (at 0 K) for the binaries. This suppression is due to downward repulsion of the $\bar{\Gamma}_{1c}(\Gamma_{1c})$ state by the $\bar{\Gamma}_{1c}(X_{3c})$ state above it. Since $\bar{\Gamma}_{1c}(\Gamma_{1c})$ is largely localized on the GaAs sublattice [Fig. 10(e)], confinement effects raise its energy substantially relative to bulk GaAs [E_0(GaAs)$=1.52$ eV]. [As the superlattice period n increases we expect the energy of this

transition to approach that for bulk GaAs.] Experimentally,[90] the most prominent photoluminescence excitation peak is at 2.12 eV (at 1.7 K) for the shortest-period superlattice studied ($n \simeq 3$). Reflectance measurements[88] (at room temperature) place this E_0 transition at ~ 2.08 eV for $n=1$, while Raman scattering experiments[89] place it at 2.15 eV. We predict two additional (weak) pseudodirect transitions, $\bar{\Gamma}_v \rightarrow \bar{\Gamma}_{4c}(X_{1c})$ at ~ 2.20 eV (i.e., *above* the disordered alloy $\Gamma_v \rightarrow X_{1c}$ transition at ~ 2.10 eV) and another at ~ 2.83 eV for $\bar{\Gamma}_v \rightarrow \bar{\Gamma}_{1c}(X_3)$.

(ii) *Indirect transitions at* $\bar{M}$. We find two X-derived states below $\bar{\Gamma}_{1c}(\Gamma_{1c})$: $\bar{M}_{5c}(X_{1c})$ at 2.09 eV [an "x-y" planar state with maximum wave-function amplitude in the interstitial volume between cations, Fig. 10(b)] and $\bar{M}_{1c}(X_{3c})$ at ~ 2.07 eV [with maximum wave-function amplitude in the interstitial volume between the anions; Fig. 10(k)]. This delocalized character suggests small confinement effects on the energies; in fact, we find these states close to the average of the calculated X_{1c} energies for GaAs and AlAs (~ 2.10 eV) or the disordered bulk *alloy* energy at X_{1c} [calculated: 2.10 ± 0.05 eV, observed 2.077 eV (Ref. 87)]. Experimentally, the lowest-energy photoluminescence peak was found at 2.01 eV ($n \sim 3$) (Ref. 90); 1.931 eV (Ref. 87, $n=1$); or ~ 2.05 eV (Ref. 80, $n \simeq 1$). The superlattice transition was found[87] 0.15 eV below the disordered alloy transition. [These data[80] imply that deviations from perfect superlattice order *raise* the energy of this transition.] We attribute the lowest emissions[90] for $n \simeq 3$ to the forbidden $\bar{M}_{5c}(X) \rightarrow \bar{\Gamma}_v$ transition; this emission exhibits[90] a long lifetime and nonexponential decay characteristic of indirect excitons. The three phonon sidebands observed[90] at lower energy exhibit both GaAs and AlAs character, consistent with the somewhat delocalized ("interstitial") wave functions at $\bar{M}_{5c}$. The emission at 1.931 eV for[87] $n=1$ could come from the $\bar{R}_{1c}(L_{1c})$ state (calculated at 1.88 eV). This is also near the weak Raman line at[89] 1.93 eV. The additional higher energy slow emission observed[90] at 2.05 eV ($n=3$) was attributed[90] to the pseudodirect $\bar{\Gamma}_{4c}(X_{1c})$ state (denoted X_z). For the case $n=1$ studied here, we find that $\bar{\Gamma}_{4c}(X_{1c})$ is higher in energy (2.20 eV). Its energy for $n=3$ will drop, placing it indeed[90] just above $\bar{M}_{5c}$.

Direct excitations into $\bar{M}_{5c}$ and $\bar{M}_{1c}$ are possible from the corresponding valence states $\bar{M}_{2v}$, $\bar{M}_{5v}$, and $\bar{M}_{4v}$ ($\simeq E_{\rm VBM} - 2.5$ eV), which are all folded from X_{5v} and are close to the calculated average of the X_{5v} states of GaAs and AlAs. We expect the $\bar{M}_v \rightarrow \bar{M}_c$ ("E_2") transitions (calculated at 4.6 ± 0.2 eV) to occur near the average energy of the E_2 transitions of GaAs and AlAs (~ 4.6 eV). Indeed, the superlattice E_2 transition was measured[88] in reflectance at ~ 4.97 eV and showed negligible confinement effects (dependence on period), consistent with the delocalized and mixed nature of the calculated wave functions.

(iii) *Transitions at* $\bar{R}$. We predict the conduction-band minimum of $(\mathrm{GaAs})_1(\mathrm{AlAs})_1$ to be at the GaAs-like $\bar{R}_{1c}(L_{1c})$ state (1.88 eV) near the corresponding state in bulk GaAs (1.81 eV). Forbidden (weak) $\bar{R}_{1c} \rightarrow \bar{\Gamma}_v$ emission could occur. The AlAs-like $\bar{R}_{4c}(L_{1c})$ state is at 2.93 eV, near the bulk AlAs L_{1c} state (~ 3 eV). Direct transitions into $\bar{R}_{1c}$ and $\bar{R}_{4c}$ are possible from the L_{3v}-derived valence-band states (in order of increasing energy) $\bar{R}_{2v}$, $\bar{R}_{4v}$, $\bar{R}_{1v}$, and $\bar{R}_{3v}$ centered at $E_{\rm VBM} - (1.1 \pm 0.1)$ eV. We hence expect the allowed $\bar{R}_v \rightarrow \bar{R}_{1c}$ transition (denoted $E_1^{\rm Ga}$) to occur at $\sim 3.0 \pm 0.1$ eV, near the bulk GaAs value (~ 3.04 eV), and the $\bar{R}_{4v} \rightarrow \bar{R}_{4c}$ transition ($E_1^{\rm Al}$) at $\sim 4.1 \pm 0.1$ eV, near the bulk AlAs value (~ 4.0 eV). For $n=1$, the $E_1^{\rm Ga}$ transition was observed[88] at 3.2 eV, but $E_1^{\rm Al}$ was not seen. Since $\bar{R}_{1c}$ ($\bar{R}_{4c}$) are strongly localized on the GaAs (AlAs) sublattice [Figs. 10(h) and 10(j)], we expect significant confinement efects, and an approach of $E_1^{\rm Ga}$ and $E_1^{\rm Al}$ to the respective bulk values of GaAs and AlAs, as the superlattice period increases. For $n=2$, $\bar{R}_{4c}$ is lowered in energy and $\bar{R}_{1c}$ is raised[76] with respect to $n=1$; their energy approaches the *average* of $E_1^{\rm Ga}$ and $E_1^{\rm Al}$ (just as in the alloy), hence, the $\bar{R}_{1v} \rightarrow \bar{R}_{1c}$ transition energy for $n=2$ is expected to be above that of $n=1$ (an increase of 0.1 eV was observed[88]).

IX. TRENDS IN STABILITY FOR THICKER MODEL [001] SUPERLATTICES

We finally examine simple models suggested by valence-force-field calculations and generalizations of the electrostatic energy calculation of Sec. VI to extract the trends to be expected. Recent work, by Van de Walle and Martin[91] for $\mathrm{Si}_n\mathrm{Ge}_n$ and by Bylander and Kleinman,[32,92] and Oshiyama and Saito,[34] for $(\mathrm{GaAs})_m(\mathrm{AlAs})_m$, indicates that extremely rapidly, as a function of superlattice thickness, AC and BC layers away from the interface in $(AC)_m(BC)_m$ greatly resemble their bulk counterparts as far as their ground-state charge densities and self-consistent electronic potentials are concerned. This conclusion is supported by, e.g., the very weak dependence of optical properties[80] and Raman scattering data[93] on m.

A. Valence-force-field calculations

Motivated by these observations, we first describe results of a simple structural model for $(AC)_m(BC)_m$ in which we distinguish A-C and B-C interlayer spacings at the A-C-B interface from those in the "bulk:" $d_G = (c/4m)(1+\varepsilon)$, $d_A = (c/4m)(1-\varepsilon)$, $d_1 = (c/4m)(1+\delta)$, $d_2 = (c/4m)(1-\delta)$, where d_G and d_A are, respectively, the Ga-As and Al-As interlayer spacings away from the interface and d_1 and d_2 are the corresponding interfacial values. The notation is illustrated for the case $m=2$ in Fig. 1(b). Minimizing the VFF strain energy with respect to ε and δ, we find for $m=1,2,3$ that (i) the equilibrium lattice constant is close to the average zinc-blende value, and (ii) successively more strain is frozen into thicker superlattices, with virtually all distortion occurring at the interfaces.

An extremely simple interpretation explains quantitatively the trends for $m=1,2,3$ VFF results for $a_s = \bar{a}$. In an $(AC)_m(BC)_m$ [001]-orientation unit cell, there are

$m-1$ layers of As atoms each coordinated by four Ga atoms and $m-1$ coordinated by four Al atoms, and two interfacial layers of As atoms coordinated by two Ga and two Al atoms. Since such layers are characteristic, respectively, of (epitaxially-constrained) GaAs, AlAs, and $(GaAs)_1(AlAs)_1$, we may write (to the extent that a given layer is coupled only to its neighboring layers) per four atoms

$$E^O_{MS}[(GaAs)_m(AlAs)_m,\bar{a}]\simeq\frac{m-1}{m}\{E^O_{MS}[GaAs,\bar{a}]+E^O_{MS}[AlAs,\bar{a}]\}+\frac{2}{m}E^O_{MS}[(GaAs)_1(AlAs)_1,\bar{a}]\ , \tag{34}$$

where all energies on the right-hand side are per cation-anion pair. This model would predict, using the VFF results for tetragonally-distorted GaAs and AlAs and $(GaAs)_1(AlAs)_1$ at $\bar{a}$, that

$$E^{\rm mod}_{MS}[(GaAs)_m(AlAs)_m,\bar{a}]=4.320-0.279/m$$

(in meV per four atoms); a least-squares fit of the form $a+b/m$ directly to the VFF results for $m=1,2,3$ yields $E^{\rm VFF}_{MS}=4.318-0.276/m$. Thus an extremely simple model accounts very well for actual VFF calculations. Identical calculations (in which we take each binary to be at its equilibrium lattice constant, ignoring the small Δa for real GaAs/AlAs) may be made for the microscopic strain (MS) contribution to the formation energy of $(GaAs)_m(AlAs)_m$, yielding (per four atoms)

$$\Delta E^O_{MS}/m=\Delta E^O_{MS}[(GaAs)_1(AlAs)_1]/m=2\sigma/m\ , \tag{35}$$

where we have identified the interfacial energy σ, using the fact that the (1,1) superlattice primitive cell consists entirely of two interfaces.

B. Electrostatic Madelung energy model

The VFF results above, together with the first-principles results[32,34,91,92] strongly support a picture in which only the regions near the interfaces in the $(AC)_m(BC)_m$ superlattice differ from their bulk counterparts. Taking, therefore, $Q_A\simeq q_A$ and $Q_B\neq q_B$ only for interfacial sites, we find for large m that $\Delta E^O_{\rm Madelung}(m,m)$ can be written (per four atoms) as

$$\Delta E^O_{\rm Madelung}/m\simeq(\Delta q)^2/mR\,[A-B(\Delta Q/\Delta q+C)^2]$$

with R an AC or BC bond length and $A=2.034$, $B=0.7722$, and $C=0.3694$. This expression predicts that, for large m, $\Delta Q/\Delta q$ must exceed 1.54 for the (m,m) superlattice to be stable. This may be written in the form (per four atoms) $\Delta E_{CE}[(AC)_m(BC)_m]=2\sigma/m$; for $\Delta Q/\Delta q=1$ it predicts $\sigma=0.293(\Delta q)^2/R$, while Eq. (23) for $m=1$ yields $\sigma=0.287(\Delta q)^2/R$, corroborating the scaling form $\Delta E^0(m,m)\simeq\Delta E^0(1,1)/m$ of Eq. (35).

C. Stability and growth of thicker superlattices

Having found the form $\Delta H^O(m,m)\simeq 2\sigma/m=\Delta H^O(1,1)/m$ per bond to emerge from two extremely different model calculations[94] for superlattice stability—one emphasizing strain effects (and yielding ΔE_{MS}) and the other Madelung charge transfer effects (and yielding approximately ΔE_{CE})—we next examine its implications for superlattice growth. For $\sigma<0$ the A-C-B interface is stable with respect to $\frac{1}{2}[A$-C-$A+B$-C-$B]$. Since $\Delta H(m,m)$ per bond scales as $1/m$, however, in thermodynamic equilibrium *if $\sigma<0$ there is no energy incentive for a thin superlattice to grow thicker* because the thicker system is less stable per bond. On the other hand [as we found above for [001] $(GaAs)_1(AlAs)_1$], *if $\sigma>0$ a thin superlattice will grow thicker* since a thick superlattice is less unstable per bond than a thin one. It is therefore clear that kinetics must be crucial in determining growth of thick, stable (or thin, unstable) superlattices like $(GaAs)_m(AlAs)_m$.

X. SUMMARY AND CONCLUSIONS

We have presented above both first-principles (pseudopotentials and all-electron) results which suggest that $(GaAs)_1(AlAs)_1$ grown in the [001] orientation is unstable both with respect to disproportionation into its zinc-blende constituents, and (Sec. IV C) with respect to disordering. We have shown that (i) semiconductor superlattices $(AC)_m(BC)_m$ exhibit, in general, a delicate competition between potentially stabilizing charge transfer (electronegativity-related) effects and destabilizing strain effects associated with imperfect accommodation of the distinct AC and BC bond lengths, which largely preserve their identities in the superlattice. As a consequence, (ii) as for other ternary compounds, in theoretically assessing delicate stability and charge-transfer questions, all structural parameters must be relaxed if a mismatch $|R_{AC}-R_{BC}|$ (theoretical *or* experimental) exists; (iii) simple models based on continuum elasticity theory and electrostatic energies (Sec. VI) are extremely useful in isolating the largely independent effects of strain and charge transfer; (iv) the electronic structure of the $(AC)_1(BC)_1$ superlattice may differ radically from those of AC and BC and a fictitious virtual crystal alloy; and (v) the issue of stability of $(AC)_m(BC)_m$ was discussed using both simple electrostatic energy models (which focus on charge-transfer effects) and valence-force-field models (which focus on strain effects) and a simple picture of stability which has as its keystone a knowledge of the interfacial energy emerged.

Many impure,[95] disordered,[96] or artificially ordered[97] semiconductor systems are manifestly *metastable* in the temperature and composition ranges in which they are routinely characterized and utilized. Such are the interstitial Mg impurity in silicon[95] (metastable at the interstitial, stable in the substitutional site at room temperature), the disordered $GaAs_xSb_{1-x}$ alloy[96] (grown in the range of thermodynamic immiscibility of GaAs and

GaSb), and *ordered* $(\text{III-V})_{1-x}(\text{IV}_2)_x$ alloys[97] (although judged by their equilibrium phase diagrams to spinodally decompose). Such metastable systems come to exist through *kinetic* rather than thermodynamic control, e.g., in nonequilibrium growth techniques[96,97] or by quenching.[95] They owe their long laboratory lifetimes and thermal stability to the existence of large activation barriers, small thermodynamic driving forces, and exceedingly low diffusion coefficients at laboratory temperatures. We suggest that this is the case for $(\text{GaAs})_1(\text{AlAs})_1$. The driving force for the ordering in $GaAlAs_2$ observed[3] at ~ 970 K remains unclear. It is possible that a *surface*-controlled mechanism is at work. Indeed, deposition of Al on the GaAs(110) surface above ~ 800 K produces a segregation effect,[98] whereby the Al is exchanged with the surface Ga to produce a GaAs layer on top of AlAs. Such fluctuating segregration sequences may produce long-range order.

APPENDIX A: VALENCE-FORCE-FIELD ESTIMATES OF MICROSCOPIC STRAIN ENERGY TERMS

In Fig. 7 we show valence-force-field predictions for the deformation energies of cubic GaAs, cubic AlAs, and unrelaxed ($\eta=1$, $u=\frac{1}{4}$) $(\text{GaAs})_1(\text{AlAs})_1$ (dashed lines). We note that all three virtually coincide at $a \simeq \bar{a} = (a_{\text{GaAs}} + a_{\text{AlAs}})/2$. This circumstance permits us to express the strain energy of the unrelaxed superlattice in terms of a superposition of those of the binary compounds (each characterized by its bulk modulus B). Shown as solid lines are curves for the binary compounds subject to tetragonal deformation due to the epitaxial (epi) constraint. We note that they, in turn, coincide with the curve for the fully-relaxed superlattice, permitting expression of the fully-relaxed superlattice deformation energy in terms of a superposition of binary curves [each characterized by the elastic modulus B^* of Eq. (21)].

More generally, the elastic properties of a given ordered ternary phase (e.g., the strain reduction upon relaxation) depend in detail on the specific structural degrees of freedom available to that phase.[40] While the analysis above was motivated by our study of $(\text{GaAs})_1(\text{AlAs})_1$, it has general validity for [001] $(AC)_1(BC)_1$ since the large Δa present in our first-principles calculation for GaAs and AlAs "simulates" the case of a physical system with large Δa, and the remarks above are based on the properties of the *structures* we have adopted for $(AC)_1(BC)_1$ and only very weakly on properties of AC or BC.

APPENDIX B: CLUSTER SUPERPOSITION DESCRIPTION OF RANDOM ALLOYS

We adopt a description[22–25] of the random disordered alloy which has proven useful for understanding structural and energetic properties of $A_xB_{1-x}C$ in terms of those of ordered stoichiometric phases $A_nB_{4-n}C_4$. In this picture the alloy is treated as a superposition of the clusters $A_nB_{4-n}C$ ($n=0$–4) spanning all possible nearest-neighbor environments in the alloy:

$$\Delta E^D(x) \simeq \sum_{n=0}^{4} P^{(n)}(x)\Delta E^{(n)} . \tag{B1}$$

For purposes of illustration and comparison with Ref. 69, we use the cluster probabilities appropriate to a perfectly random alloy, i.e., $P^{(n)}(x)=\binom{4}{n}x^n(1-x)^{4-n}$. Ignoring volume dependence of cluster-formation energies (appropriate to lattice-matched clusters), the cluster-formation energies $\Delta E^{(n)}$ become fixed numbers (zero for the clusters $n=0$ and $n=4$). We evaluate the excess Madelung energy for clusters $n=1,2,3$ using ordered structures predicted by the Landau-Lifshitz theory of structural phase transitions for the fcc alloy phases of interest.[20,39,40] We have already evaluated $\Delta E^{(2)}_{\text{Madelung}}$ [Eq. (23)] for $(AC)_1(BC)_1$; for $n=1$ and 3 we use the Luzonite A_3BC_4 and AB_3C_4 structures, respectively. We find, performing calculations identical to those for $(AC)_1(BC)_1$ (with a bond length R common to all structures) that $\Delta E^{(1)}_{\text{Madelung}} = \Delta E^{(3)}_{\text{Madelung}} = \frac{3}{4}\Delta E^{(2)}_{\text{Madelung}}$. These relations are valid for any ΔQ, but assume the same ΔQ for all ordered phases, although this is not likely to be valid for real systems. Performing the sum in Eq. (B1), we find[71] per four atoms

$$\begin{aligned} \Delta E^D_{\text{Madelung}}(x) &= 3\Delta E^O_{\text{Madelung}}(1,1)x(1-x) , \\ \Delta E^{(n)}_{\text{Madelung}}(x_n) &= 4\Delta E^O_{\text{Madelung}}(1,1)x_n(1-x_n) , \end{aligned} \tag{B2}$$

where $x_n = n/4$ for $n=0,1,2,3,4$.

The treatment of the random alloy by van Schilfgaarde, Chen, and Sher[69] is based on a direct lattice sum with truncation of the electrostatic energy sums at nearest neighbors for cation-cation, anion-cation, and anion-anion interactions and use of the binomial coefficients $P^{(n)}(x)$ to evaluate the site probabilities and conditional probabilities which arise in this approach. In their calculation a prefactor of $\frac{1}{2}$ was incorrectly omitted from their anion-anion lattice sum.[72] Correcting for this, their result (given[69] for $\Delta Q=\Delta q$) is per four atoms

$$\Delta E^D_{\text{Madelung}}(x=\tfrac{1}{2}) = 0.434(\Delta Q)^2/R , \tag{B3}$$

compared with our result [Eq. (B2), where $\Delta E^O_{\text{Madelung}}(1,1)$ is given by Eq. (23)], evaluated for $\Delta Q=\Delta q$:

$$\Delta E^D_{\text{Madelung}}(x=\tfrac{1}{2}) = 0.431(\Delta Q)^2/R . \tag{B4}$$

Comparing (B3) with (B4) shows that the Madelung energy of a random alloy can be calculated either by a superposition of local clusters [Eq. (B4)] or by direct lattice sums [Eq. (B3)].

van Schilfgaarde *et al.*[69] observed that, "most alloy calculations are carried out in a cluster approximation, which divides the lattice into clusters and assigns an energy to each cluster that is taken to be independent of the surrounding clusters . . ." and speculate that, "because the Coulomb interaction is long ranged on the scale of a bond length, small clusters may in fact depend strongly on the surroundings. Virtually all present-day calculations embedded clusters in either a virtual crystal or a supercell to obtain cluster energies. This work indicates that in many cases such an approximation may be

quite poor, particularly for small clusters. The smallest cluster size that is reasonably configuration independent has not yet been determined." We note that the extremely close agreement between the effective Madelung constant for a disordered alloy obtained via a superposition-of-clusters approach and their truncation of the Madelung energy [Eqs. (B3) and (B4)] shows that this speculation is incorrect.

Analogous superposition procedures may be carried out for on-site Coulomb contributions for the disordered alloy (and give results identical to those of van Schilfgaarde *et al.*). For each atom α in each cluster the Coulomb energy varies as

$$E_\alpha(q) \simeq E_\alpha(0) - \varepsilon_\alpha q + \tfrac{1}{2} U_\alpha q^2 + \cdots .$$

When evaluating the on-site Coulomb contribution to the formation energy of a cluster, the terms in $E_\alpha(0)$ disappear since there are as many A, B, and C atoms in the cluster as in equivalent amounts of AC and BC; those in ε cancel similarly. The net on-site contributions to the formation energy per cation-anion pair are extremely simple for $\Delta Q = \Delta q$: $\Delta E_{\rm OS}^{(0)} = \Delta E_{\rm OS}^{(4)} = 0$, $\Delta E_{\rm OS}^{(1)} = \Delta E_{\rm OS}^{(3)} = -3U_C(\Delta Q)^2/32$, and $\Delta E_{\rm OS}^{(2)} = -U_C(\Delta Q)^2/8$. Summing these cluster on-site energies weighted with the binomial coefficients for composition $x = \frac{1}{2}$, one finds for the random alloy $E_{\rm OS}^D = -3U_C(\Delta Q)^2/32$, which agrees with the results of van Schilfgaarde *et al.*, except for the much simpler notation resulting from evaluating formation energies rather than energies referred to the virtual crystal. Thus

$$\begin{aligned} \Delta E_{\rm OS}^D(x) &= 3\,\Delta E_{\rm OS}^O(1,1)x(1-x) , \\ \Delta E_{\rm OS}^{(n)}(x_n) &= 4\,\Delta E_{\rm OS}^O(1,1)x_n(1-x_n) . \end{aligned} \tag{B5}$$

[1] See, for example, *Modulated Structure Materials*, edited by T. Tsakalakos (Martin Nijhoff, Dordrecht, 1985). For more general reviews of superlattice properties, see the Proceedings of the 12th Annual Conference on the Physics and Chemistry of Semiconductor Interfaces [J. Vac. Sci. Technol. B **3**, No. 4 (1985)].

[2] A. C. Gossard, P. M. Petroff, W. Weigmann, R. Dingle, and A. Savage, Appl. Phys. Lett. **29**, 323 (1976); P. M. Petroff, A. C. Gossard, W. Weigmann, and A. Savage, J. Cryst. Growth **44**, 5 (1978); P. M. Petroff, A. C. Gossard, A. Savage, and W. Weigmann, *ibid.* **46**, 172 (1979); A. C. Gossard, Thin Solid Films **57**, 3 (1979); P. M. Petroff, A. C. Gossard, and W. Weigmann, Appl. Phys. Lett. **45**, 620 (1984); P. M. Petroff, A. Y. Cho, F. K. Reinhart, A. C. Gossard, and W. Weigmann, Phys. Rev. Lett. **48**, 170 (1982); P. M. Petroff, Nature **316**, 389 (1985); N. Sano, H. Kato, M. Nakayama, S. Chika, and H. Terauchi, Jpn. J. Appl. Phys. **23**, L640 (1984).

[3] T. S. Kuan, T. F. Kuech, W. I. Wang, and E. L. Wilkie, Phys. Rev. Lett. **54**, 201 (1985).

[4] Y. Hirayama, Y. Ohmori, and H. Okamoto, Jpn. J. Appl. Phys. II **23**, L488 (1984).

[5] T. Fukui and H. Saito, Jpn. J. Appl. Phys. **23**, L521 (1984); **24**, L774 (1985).

[6] T. S. Kuan, W. I. Wang, and E. L. Wilkie, Appl. Phys. Lett. **51**, 51 (1987). See also, M. A. Shahid, S. Mahajan, D. E. Laughlin, and H. M. Cox, Phys. Rev. Lett. **58**, 2567 (1987) for [111] superlattice ordering.

[7] (a) H. Nakayama and H. Fujita in *Gallium Arsenide and Related Compounds 1985*, edited by M. Fujimoto, Inst. Phys. Conf. Ser. No. **79** (Hilger, Boston, 1986), p. 289; (b) Y. Matsui, H. Hayashi, and K. Yoshida, Appl. Phys. Lett. **48**, 1060 (1986).

[8] H. R. Jen, M. J. Cherng, and G. B. Stringfellow, Appl. Phys. Lett. **48**, 1603 (1986).

[9] A. Gomyo, T. Suzuki, K. Kobayashi, S. Kawatu, and I. Hindo, Appl. Phys. Lett. **50**, 673 (1987).

[10] P. D. Dernier, D. E. Moncton, D. B. McWhan, A. C. Gossard, and W. Weigmann, Bull. Am. Phys. Soc. **22**, 293 (1977); J. L. Merz, A. S. Barker, and A. C. Gossard [Appl. Phys. Lett. **31**, 117 (1977)] estimate that only 20–30% of cation sites are disordered in $(GaAs)_1(AlAs)_1$.

[11] At typical growth temperature of 600 °C diffusion lengths in $(AlAs)_m(GaAs)_m$ are well below one monolayer. See R. Dingle, A. C. Gossard, and W. Weigmann, Bull. Am. Phys. Soc. **21**, 367 (1976); L. L. Chang and A. Koma, Appl. Phys. Lett. **29**, 138 (1976); Y. Hirayama, Y. Horikoshi, and H. Okamoto, Jpn. J. Appl. **23**, 1568 (1984).

[12] 560–570 °C: see P. M. Petroff, A. C. Gossard, W. Weigmann, and A. Savage, J. Cryst. Growth **44**, 5 (1978).

[13] An ordering temperature of $\sim$610 °C is given in Ref. 12. Note, however, that diffusion of, e.g., Zn [W. D. Laidig, N. Holonyak, Jr., M. D. Camras, K. Hess, J. J. Coleman, P. D. Dapkus, and J. Bardeen, Appl. Phys. Lett. **38**, 776 (1981); W. D. Laidig, J. W. Lee, P. K. Chiang, L. W. Simpson, and S. M. Bedair, J. Appl. Phys. **54**, 6382 (1983); J. W. Lee and W. D. Laidig, J. Electron. Mater. **13**, 147 (1984)], Si [J. J. Coleman, P. D. Dapkus, C. G. Kirkpatrick, M. D. Camras, and N. Holonyak, Jr., Appl. Phys. Lett. **40**, 904 (1982); K. Meehan, N. Holonyak, Jr., J. M. Brown, M. A. Nixon, P. Gavrilovic, and R. D. Burnham, *ibid.* **45**, 549 (1984)], or Be [M. Kawabe, N. Shimizu, F. Hasegawa, and Y. Nannichi, Appl. Phys. Lett. **46**, 849 (1985)] into $(GaAs)_m(AlAs)_m$ superlattices appears to catalyze the disordering, yielding lower disordering temperatures ($\lesssim$550 °C).

[14] ΔS for ordered or disordered phases will have electronic and vibrational contributions; for the disordered phase there is an additional configurational entropy contribution. Insofar as electronic and vibrational contributions to S are expected to be very similar for either the ordered compound or the substitutionally disordered alloy and the binary constituents, we will henceforth retain only the configurational contribution to ΔS^D and set $\Delta S^\alpha = 0$ and $\Delta S^D \simeq -k_B[(1-x)\ln(1-x) + x\ln x]$ per cation.

[15] R. Hultgren, P. D. Desai, D. T. Hawkins, M. Gleiser, and K. K. Kelley, *Selected Values of the Thermodynamic Properties of Binary Alloys* (American Society for Metals, Metals Park, Ohio, 1973).

[16] A. Zunger, Appl. Phys. Lett. **50**, 164 (1987).

[17] M. B. Panish and M. Ilegems, Prog. Solid State Chem. **7**, 39 (1972).

[18] G. B. Stringfellow, J. Cryst. Growth **27**, 21 (1974); J. Phys. Chem. Solids **23**, 665 (1972).

[19] J. L. Martins and A. Zunger, Phys. Rev. Lett. **56**, 1400 (1986).

[20] J. L. Martins and A. Zunger, J. Mater. Res. **1**, 523 (1986).

[21] S.-H. Wei and A. Zunger, Phys. Rev. Lett. **56**, 2391 (1986); Phys. Rev. B **35**, 2340 (1987).

[22] A. A. Mbaye, L. G. Ferreira, and A. Zunger, Phys. Rev.

Lett. **58**, 49 (1987).

[23]L. G. Ferreira, A. A. Mbaye, and A. Zunger, Phys. Rev. B **35**, 6475 (1987).

[24](a) L. G. Ferreira, A. A. Mbaye, and A. Zunger (unpublished); (b) S.-H. Wei, A. A. Mbaye, L. G. Ferreira, and A. Zunger, Phys. Rev. B **36**, 4163 (1987).

[25]G. P. Srivastava, J. L. Martins, and A. Zunger, Phys. Rev. B **31**, 2561 (1985).

[26]M. Ettenberg and R. J. Paff, J. Appl. Phys. **41**, 3926 (1970). See also, *Semiconductors,* Vol. 17e of *Landolt-Börnstein, New Series,* edited by O. Madelung, M. Schulz, and H. Weiss (Springer-Verlag, Berlin, 1982), Secs. 2.10.3 and 2.6.3.

[27]P. M. Petroff, *Layered Structures and Epitaxy, Boston, 1985,* edited by J. M. Gibson, G. C. Osbourn, and R. M. Tromp, Mater. Res. Soc. Symp. Proc. No. **56** (MRS, Pittsburgh, PA, 1986), p. 19.

[28]J. C. Phillips, J. Vac. Sci. Technol. **19**, 545 (1981).

[29]A. Ourmazd and J. C. Bean, Phys. Rev. Lett. **55**, 765 (1985).

[30]A. B. Chen and A. Sher, Phys. Rev. B **32**, 3695 (1985).

[31]A. Zur and T. C. McGill, J. Vac. Sci. Technol. B **3**, 1055 (1985).

[32]D. M. Bylander and L. Kleinman [Phys. Rev. B **36**, 3229 (1987)] used semirelativistic norm-conserving pseudopotentials and a mixed-basis description with two s and two p Gaussian orbitals per atom and plane waves with a kinetic-energy cutoff of ~ 11.6 Ry. Their value $\Delta H^O(1,1) = +15.5$ meV corrects their unconverged earlier value of 9.2 meV [Phys. Rev. B **34**, 5280 (1986)].

[33]S. Ciraci and I. P. Batra, Phys. Rev. Lett. **58**, 2114 (1987); these authors used the Bachelet-Hamann-Schlüter parametrizations [Phys. Rev. B **26**, 4199 (1982)] and a plane-wave basis of ~ 1200 plane waves. They relaxed all bonds and lattice parameters. I. B. Batra, S. Ciraci, and J. S. Nelson [J. Vac. Sci. Technol. B **5**, 1300 (1987)] examine the electronic structure of $(GaAs)_m(AlAs)_m$ for $m \leq 4$. K. Kunc and I. P. Batra [Phys. Rev. Lett. (to be published)] treat approximately the energy of a disordered $Ga_{0.5}Al_{0.5}As$ alloy and the quantities $\Delta H^O(2,2)$ and $\Delta H^O(3,3)$, using a norm-conserving pseudopotential description, the Ceperley-Alder exchange correlation, but without structural relaxation from the average lattice constant ($\Delta a \simeq 0.03$ Å).

[34]A. Oshiyama and M. Saito, Phys. Rev. B **36**, 6156 (1987). These authors used the Ceperley-Alder exchange-correlation potential, a kinetic-energy cutoff of 12.6 Ry, and lattice constant relaxation only. They find $\Delta a = 0.116$ Å, suggesting that relaxation of c/a and u would lower $\Delta H^O(1,1)$ by several meV per four atoms.

[35]T. Ito, Phys. Status Solidi B **135**, 493 (1986); *Proceedings of the 18th International Conference on the Physics of Semiconductors,* edited by O. Engstrom (World-Scientific, Singapore, 1987), p. 1225.

[36]D. M. Wood, S. H. Wei, and A. Zunger, Phys. Rev. Lett. **58**, 1123 (1987). An inconsistent choice for the core-level grid in the LAPW calculations reported in this paper gave a value for ΔH^0 about 10 meV too high. This error is corrected in the present paper.

[37]J. E. Jaffe and A. Zunger, Phys. Rev. Lett. **51**, 662 (1983); Phys. Rev. B **29**, 1882 (1984).

[38]M. Hansen and K. Anderko, *Constitution of Binary Alloys* (McGraw-Hill, New York, 1958), p. 200.

[39]L. D. Landau and E. M. Lifshitz, *Statistical Physics* (Pergamon, Oxford, 1969), Chap. 14; A. G. Khachaturyan, *Theory of Structural Transformations in Solids* (Wiley, New York, 1983).

[40](a) A. A. Mbaye, D. M. Wood, and A. Zunger, Phys. Rev. B (to be published); (b) A. A. Mbaye, D. M. Wood, and A. Zunger, Appl. Phys. Lett. **49**, 782 (1986).

[41]J. H. van der Merwe, J. Appl. Phys. **34**, 123 (1963); J. W. Matthews and A. E. Blakeslee, J. Cryst. Growth **27**, 118 (1974); R. People and J. C. Bean, Appl. Phys. Lett. **47**, 322 (1985).

[42]J. Ihm, A. Zunger, and M. L. Cohen, J. Phys. C **12**, 4409 (1979).

[43]J. P. Perdew and A. Zunger, Phys. Rev. B **23**, 5048 (1981); D. M. Ceperley and B. J. Alder, Phys. Rev. Lett. **45**, 566 (1980).

[44]S.-H. Wei and H. Krakauer, Phys. Rev. Lett. **55**, 1200 (1985), and references therein.

[45]L. Hedin and B. I. Lundqvist, J. Phys. C **4**, 2064 (1971).

[46]G. P. Kerker, J. Phys. C **13**, L189 (1980), similar in construction to the analytically-continued pseudopotentials of A. Zunger and M. L. Cohen, Phys. Rev. B **20**, 4082 (1979). We used ground-state configurations to generate the $l=0$ and $l=1$ pseudopotentials. For Ga and Al we used the configuration $s^{1.5}p^{0.5}d^1$ and for As $s^2p^2d^1$ to generate the $l=2$ pseudopotential.

[47]D. J. Chadi and M. L. Cohen, Phys. Rev. B **8**, 5747 (1973).

[48]The two Chadi-Cohen points $\mathbf{k}_1=(\frac{1}{4},\frac{1}{4},\frac{1}{4})$ (of weight $\frac{1}{4}$) and $\mathbf{k}_2=(\frac{1}{4},\frac{1}{4},\frac{3}{4})$ (of weight $\frac{3}{4}$), expressed in terms of the primitive translation vectors $\mathbf{b}_1=(2\pi/a)(-\hat{\mathbf{x}}+\hat{\mathbf{y}}+\hat{\mathbf{z}})$ (and cyclic permutations) of the lattice reciprocal to the fcc direct lattice, for the (1,1) superlattice become (each with equal weight) $\mathbf{k}_1=(0,\frac{1}{4},\frac{1}{4})$ and $\mathbf{k}_2=(\frac{1}{2},\frac{1}{4},\frac{1}{4})$ (expressed in terms of the primitive translation vectors of the tetragonal reciprocal lattice, $\mathbf{b}_1=(2\pi/a)(\hat{\mathbf{x}}+\hat{\mathbf{y}})$, $\mathbf{b}_2=(2\pi/a)(-\hat{\mathbf{x}}+\hat{\mathbf{y}})$, and $\mathbf{b}_3=(2\pi/a)\hat{\mathbf{z}}/\eta$ for $\eta \simeq 1$.

[49]P. N. Keating, Phys. Rev. **145**, 637 (1966).

[50]R. M. Martin, Phys. Rev. B **1**, 4005 (1970).

[51]J. L. Martins and A. Zunger, Phys. Rev. B **30**, 6217 (1984).

[52]For $(GaAs)_1(AlAs)_1$ bond-bending force constants for bonds not present in the binary constituents were taken as simple averages of the reciprocals of the binary force constants (a reasonable procedure since these materials are elastically very similar).

[53]The lattice parameter of GaAs at 300 K is 5.653 25 Å [J. B. Mullin, B. W. Straughan, C. M. H. Driscoll, and A. F. W. Willoughby, in *Fifth International Symposium on GaAs and Related Compounds,* edited by J. Bok, Inst. Phys. Conf. Ser. No. **24**, (IOP, London, 1975), p. 275] and the linear thermal expansion is 6.86×10^{-6} K^{-1}. The lattice parameter of AlAs is 5.660 Å [W. B. Pearson, *A Handbook of Lattice Spacings and Structures of Metals and Alloys* (Pergamon, Oxford, 1967)].

[54]The elastic constants C_{11} and C_{12} for AlAs have not been measured, but were estimated using empirical relations and values from other compounds. This gave $C_{11}=12.5\times10^{11}$ dyn/cm^2 and $C_{12}=5.34\times10^{11}$ dyn/cm^2 [J. D. Wiley, in *Semiconductors and Semimetals,* edited by R. K. Willardson, and A. C. Beer (Academic, New York, 1975)]. The measured values for GaAs are $C_{11}=12.11\times10^{11}$ dyn/cm^2 and $C_{12}=5.48\times10^{11}$ dyn/cm^2 extrapolated to $T=0$ K [R. J. Cottam and G. A. Saunders, J. Phys. C **6**, 2105 (1973)]. These values give B(AlAs)=77.3 GPa and B(GaAs)=76.9 GPa.

[55]The cohesive energy is obtained by subtracting from the measured formation enthalpies of AlAs and GaAs the cohesive energies of the elemental solids [29.3±1.2 and 19.5±0.6 kcal/mole, respectively, from compilation by O. Ku-

baschewski and C. B. Alcock, *Metallurgical Thermochemistry*, 5th ed. (Pergamon, Oxford, 1979), pp. 268 and 286]. The elemental cohesive energies are as follows: Al, 78.1; Ga, 64.8; and As, 68.2 kcal/mole, from L. Brewer, Lawrence Berkeley Laboratory Report No. 3720 (1975), quoted by C. Kittel, in *Introduction to Solid State Physics*, 6th ed. (Wiley, New York, 1986). This gives $E_c(\text{AlAs}) = +29.3 + 78.1 + 68.2 = 175.6$ kcal/mole or 3.81 eV/atom and $E_c(\text{AlAs}) = +19.5 + 64.8 + 68.2 = 152$ kcal/mole or 3.31 eV/atom. We neglect the small zero-point energy and the thermal correction to the enthalpy from 298 to 0 K.

[56]S. Froyen and M. L. Cohen, Phys. Rev. B **28**, 3258 (1983), give $\Delta a = 0.071$ Å.

[57]J. Ihm and J. Joannopoulos, Phys. Rev. B **24**, 4191 (1981).

[58]See, for example, R. H. Parmenter, Phys. Rev. **97**, 587 (1955); L. Nordheim, Ann. Phys. (Leipzig) **9**, 607 (1931); **9**, 641 (1931).

[59]The interaction parameter Ω has not been measured directly in semiconductor alloys. Rather, it was inferred from fitting the liquidus-solidus line to a simple thermodynamic model (see Refs. 17 and 18). V. T. Bublik and V. N. Leikin [Ref. 60(a)] inferred from diffuse x-ray scattering data a value $\Omega = 1.6$ kcal/1-cation mole. Indirect estimates based on the high-temperature phase diagram give $\Omega \simeq 0$ [L. M. Foster, J. E. Scardefield, and J. F. Woods, J. Electrochem. Soc. **119**, 765 (1972); G. B. Stringfellow, J. Phys. Chem. Solids **34**, 1749 (1973)]; $\Omega = -0.5$ kcal/mole at 1000 °C (Ref. 17); and at 700 °C [H. C. Casey and M. B. Panish, in *Heterostructure Lasers* (Academic, New York, 1978)], $\Omega = -3.89 + 0.004\,T$, for $123 \leq T \leq 1273$ K.

[60](a) V. T. Bublik and V. N. Leikin, Phys. Status Solidi A **46**, 365 (1978); (b) A. Balzarotti, P. Letardi, and N. Motta, Solid State Commun. **56**, 471 (1985).

[61]There are several reasons $\Delta E_{\text{res}} \neq 0$: (1) Bond properties (length, force constants) change in the ternary environment because of charge-transfer effects (e.g., between Ga and Al) not present in the pure binary compounds; (2) in our calculations, experimental (rather than first-principles) bond-stretching and -bending force constants were used in conjunction with theoretical bond lengths, leading to imperfect description of strain contributions in first-principles results; (3) first-principles energies contain contributions from interactions of longer range than the first- and second-nearest neighbor (bond stretching and bending, respectively) interactions present in VFF, and (4) first-principles total energies are generally anharmonic in atomic displacements (unlike the regime of validity of VFF). Because we believe reason (1) to be most important, we categorize ΔE_{res} as chemical in origin.

[62]A Baldereschi, F. Meloni, and M. Serra, Nuovo Cim. **20**, 1643 (1983).

[63]S. Massidda, B. I. Min, and A. J. Freeman, Phys. Rev. B **35**, 9871 (1987).

[64]K. Akimoto, Y. Mori, and C. Kojima, Phys. Rev. B **35**, 3799 (1987).

[65]W. E. Pickett, S. G. Louie, and M. L. Cohen, Phys. Rev. B **17**, 815 (1978).

[66]E. Caruthers and P. J. Lin-Chung, Phys. Rev. Lett. **38**, 1543 (1977); Phys. Rev. B **17**, 2705 (1978); J. Vac. Sci. Technol. **15**, 1459 (1978).

[67]U. Pietsch, Phys. Status Solidi B **134**, 21 (1986); **128**, 439 (1985).

[68]W. I. Wang [Appl. Phys. Lett. **58**, 3244 (1985)] suggested that the net Madelung formation energy is negative, failing to distinguish ΔQ from Δq [Eq. (23)].

[69]M. van Schilfgaarde, A.-B. Chen, and A. Sher. Phys. Rev. Lett. **57**, 1149 (1986); **59**, 2614 (1987). They use the notation $\Delta Z = \frac{1}{2}\Delta Q$. See also, S.-H. Wei, Phys. Rev. Lett. **59**, 2613 (1987), who corrected their expression.

[70]The condition $\Delta Q = \Delta q$, while not necessary, removes terms in $(\varepsilon_A - \varepsilon_B)(\Delta Q - \Delta q)$, $\bar{U}[(\Delta Q)^2 - (\Delta q)^2]$, $\bar{Q}(U_A - U_B)(\Delta Q - \Delta q)$, and, for A_3BC and AB_3C clusters, "nonadditive" terms in $[\bar{U} - \frac{1}{2}(U_A - U_B)]$ which would cause the on-site contribution ΔE_{OS}^{D} to depend nonparabolically on x in Eq. (26). [Here for the $A_{4-n}B_nC_4$ structure we define $\bar{U} = \frac{1}{4}(4-n)U_A + \frac{1}{4}nU_B$.] This approximation was made in the interest of simplicity—the equation for the on-site Coulomb term would be much longer without it.

[71]This simple relation between Madelung formation energies between ordered phases of differing stoichiometry is identically obeyed when $n = 2$, 1, and 3 clusters are drawn from CuAu-I ABC_2, Luzonite A_3BC_4 and Luzonite AB_3C_4, respectively. It is very closely obeyed for other possible ordered structures, e.g., chalcopyrite $A_2B_2C_4$ for $n = 2$ and famatinite A_3BC_4 and AB_3C_4 (see Ref. 40) for $n = 1$ and 3. See Appendix B.

[72]In Ref. 69 the next-nearest-neighbor (like-charge) contribution to the Madelung energy of the random alloy [their Eq. (6)] was double-counted, making the ordered phase appear spuriously stable by comparison. The correct next-nearest-neighbor term should be $\frac{6}{16}(\frac{8}{3})^{-1/2}e^2/d$.

[73]For the case of Si_nGe_n, see T. P. Pearsall, J. Bevk, L. C. Feldman, A. Ourmazd, J. M. Bonar, and J. P. Mannaerts, Phys. Rev. Lett. **58**, 729 (1987).

[74]S. Froyen, D. M. Wood, and Alex Zunger, Phys. Rev. B **36**, 4547 (1987).

[75]N. E. Christensen, E. Molinari, and G. B. Bachelet, Solid State Commun. **56**, 125 (1985).

[76]N. Hamada and S. Ohnishi, Superlatt. Microstruct. **3**, 301 (1987).

[77]W. Andreoni and R. Car, Phys. Rev. B **21**, 3334 (1980).

[78]H. Kamimura and T. Nakayama (private communication); T. Nakayama and H. Kamimura, J. Phys. Soc. Jpn. **54**, 4726 (1985).

[79]A. Blancha, H. Prestiny, and M. Cardona, Phys. Status Solidi B **126**, 11 (1984).

[80]A. Ishibashi, Y. Mori, M. Itabashi, and N. Watanabe, J. Appl. Phys. **58**, 2691 (1985).

[81]H. J. Lee, L. Y. Juravel, J. C. Woolley, and A. J. Springthorpe, Phys. Rev. B **21**, 659 (1980).

[82]H. Temkin and V. G. Keramidas, J. Appl. Phys. **51**, 3269 (1980).

[83]D. D. Sell, in *Proceedings of the 11th International Conference on Physics of Semiconductors, Warsaw* (Polish Scientific, Warsaw, 1972), p. 1023.

[84]A. B. Chen and A. Sher, Phys. Rev. B **23**, 5360 (1981).

[85]J. E. Bernard, S.-H. Wei, D. M. Wood, and A. Zunger, Appl. Phys. Lett. (to be published).

[86]J. E. Bernard and A. Zunger, Phys. Rev. B **36**, 3199 (1987); **34**, 5992 (1986).

[87]T. Isu, D. S. Jiang, and K. Ploog, Appl. Phys. A **43**, 75 (1987).

[88]M. Garriga, M. Cardona, N. E. Christensen, P. Lautenschlager, T. Isu, and K. Ploog, Phys. Rev. B **36**, 3254 (1987).

[89]M. Cardona, T. Suemoto, N. E. Christiansen, T. Isu, and K. Ploog, Phys. Rev. B **36**, 5906 (1987).

[90]E. Finkman, M. D. Sturge, M. H. Meynadier, R. E. Nahory,

M. C. Tamargo, D. M. Hwang, and C. C. Chang, J. Lumin. (to be published).

[91]C. G. Van de Walle and R. M. Martin, J. Vac. Sci. Technol. B **3**, 1256 (1985).

[92]D. Bylander and L. Kleinman, Phys. Rev. Lett. **59**, 2091 (1987).

[93]A. Ishibashi, M. Itabashi, S. Kawado, N. Watanabe, Y. Mori, and K. Kaneko, Phys. Rev. B **33**, 2887 (1986).

[94]Recent calculations by Bylander and Kleinman (Ref. 88) indicate that this scaling form is not correct for $m \leq 3$.

[95]J. E. Baxter and G. Ascarelli, Phys. Rev. B **7**, 2630 (1973); S. Froyen and A. Zunger, *ibid.* **34**, 7451 (1986).

[96]R. M. Cohen, M. M. Cherng, R. E. Benner, and G. B. Stringfellow, J. Appl. Phys. **57**, 4817 (1985).

[97]S. I. Shah, B. Kramer, S. A. Barnett, and J. E. Greene, J. Appl. Phys. **59**, 1482 (1986).

[98]L. J. Brillson, R. Z. Bachrach, R. S. Bauer, and J. McMeanmin, Phys. Rev. Lett. **42**, 397 (1979); A. Zunger, Phys. Rev. B **24** 4372 (1981).

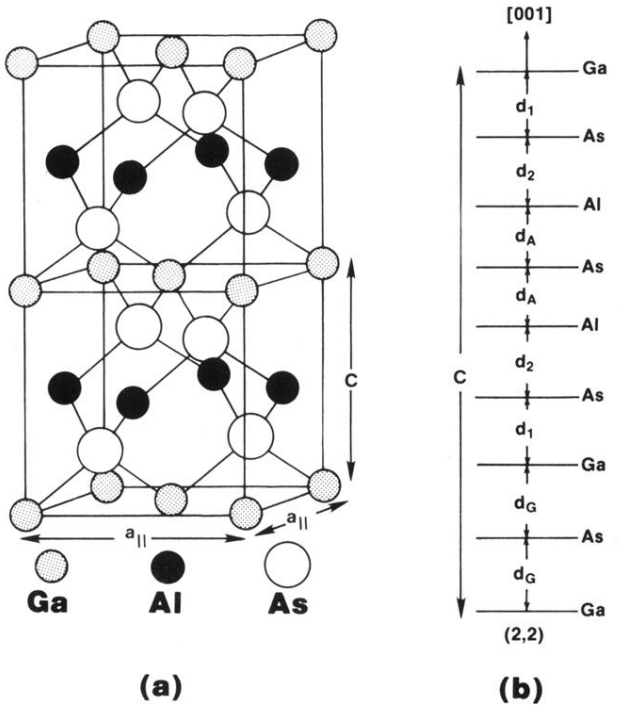

FIG. 1. (a) Two stacked unit cells of the [001]-orientation $(AC)_1(BC)_1$ superlattice; (b) structural parameters of simple model (Sec. VIII A) for $(AC)_m(BC)_m$ illustrated for $m=2$.